TÜBİTAK

Turkish Journal of Biology

http://journals.tubitak.gov.tr/biology/

Review Article

Turk J Biol
(2017) 41: 673-699

doi:10.3906/biy-1705-31

Hybrid nanomaterial: biocolloidals

Numan GÖZÜBENLİ[1,*], Emir YASUN[2], Nihat DİLSİZ[3]

[1]Department of Molecular Biology and Genetics, Faculty of Arts and Sciences, Harran University, Şanlıurfa, Turkey

[2]Department of Mechanical Engineering and Biological Nanostructures Laboratory, California NanoSystems Institute (CNSI), University of California, Santa Barbara, CA, USA

[3]Department of Molecular Biology and Genetics, Faculty of Engineering and Natural Sciences, İstanbul Medeniyet University, İstanbul, Turkey

Received: 10.05.2017 • **Accepted/Published Online:** 04.08.2017 • **Final Version:** 10.11.2017

Abstract: Nanomaterials-based diagnostics have tremendous advantages over other conventional diagnostic systems in terms of sensitivity, specificity, and portability owing to the unique intrinsic properties of nanomaterials. Thus, there is a substantial need to develop and employ a broad spectrum of nanomaterials for biological and diagnostic applications. In this review, we focus on nanomaterials-assisted disease diagnosis utilizing different techniques such as photoluminescence, colorimetry, fluorescence, electrochemistry, microarray methods, surface plasmon resonance, and surface-enhanced Raman spectroscopy. In these techniques, different nanomaterials, including but not limited to gold and silver materials, metal oxides, and semiconductors, were employed according to their all-purpose chemical and physical properties. As the new properties of nanomaterials are discovered, their contributions to nanobiotechnology applications are vastly increased. In this review, the features of the selected nanobiomaterials, biological tag-modified nanomaterials, and their outstanding applications for the detection of specific biotargets have been summarized according to the latest studies. Nanomaterials contribute to the fields of photo/chemotherapy and biomedical imaging in particular, since all the biological events happen within this size range and beneficiary roles of nanoparticles (NPs) are countless in biomedical applications due to their unique physical and chemical properties. However, due to the necessity of specificity and selectivity, there is a clear ambition to study bioconjugation of NPs to increase the efficiency of the targeted biological applications. Thus, the combination of the specificity and the intrinsic properties of biohybrid NPs facilitate diagnostic and therapeutic applications.

Key words: Nanocolloids, bioconjugation, photoluminescence, bioplasmonic structures, medical diagnosis, bioimaging, biotechnology, theranostics, biological tags, optoelectronic

1. Introduction

Nanomaterials synthesized from their precursors using different techniques demonstrate many different properties compared to their bulk materials. These properties have increased the motivation for developing and modifying these nanomaterials to be used in current technology fields such as catalyst systems, electromechanical systems, biological systems, optical sensors, displays, and electronic circuits (McBride et al., 2006). On the other hand, the impact of these nanoparticles (NPs) in different fields also requires improved techniques to fabricate high throughput and precise (monodisperse) nanomaterials. The development of the electronics industry has also led to the improvement of nanofabrication techniques such as photolithography. Because of high resolution and high throughput, recent photolithography improvements have guided fabrication of patterns with a sensitivity of several hundred nanometers in size. However, patterns on a sub-100-nm scale are not applicable by classical photolithography technique due to the diffraction limitation of light, backscattering from the substrate, and difficulty in developing master molds. Currently, achieving precise master molding has increased research interest in more advanced lithography techniques. For example, in dip-pen nanolithography, a high refractive index liquid is used between an imaging lens and other tools such as photoresists, e-beams, focused ion beams, and scanning probes. There are also two prominent methods for fabricating colloidal photonic crystals (André et al., 2016) and periodic plasmonic nanostructures (Malaczewska, 2014; Madden et al., 2015; Mahyad et al., 2015; Mansur et al., 2015; Del Mercato et al., 2016): electron-beam lithography and focused ion-beam milling. In addition to numerous similar nanooptical applications, the improvement of

* Correspondence: gnuman@harran.edu.tr

plasmonic structure and photonic crystals based on integrated optical circuits has been mostly hindered by sophisticated top-down nanofabrication techniques. However, high yield for large-area fabrication is still an important challenge with these top-down techniques. Conversely, bottom-up techniques, including colloidal self-assembly and subsequent templating nanofabrication techniques, provide a much more practical and cost-effective method compared to nanolithography. Various colloidal self-assembly techniques, such as spin-coating (Ackerson, 1990; Cheng et al., 2011; Im et al., 2011; Muller and Batchelli, 2013), gravity sedimentation (Blanco et al., 2000; Muller and Batchelli, 2013), electrostatic repulsion (Cheng et al., 2011; Im et al., 2011; Zu et al., 2011; Kumar et al., 2014; Rodio et al., 2016), template-assisted assembly (Kang et al., 2015; Logeswari et al., 2015; Luo et al., 2015; Garrido et al., 2016; Li et al., 2016), physical confinement (Prorok et al., 2014; Garrido et al., 2016), layer-by-layer growth (Pieranski, 1983; Trau et al., 1996; Bardosova et al., 2010), shear-aligned assembly (Zhong et al., 2003), electromagnetic field-assisted crystallization (Herold et al., 2012; Wagner et al., 2014), and capillary force-based self-assembly (Kaombe and Hagg, 2014; Khiyami et al., 2014; Karatutlu et al., 2015; Kira et al., 2016), have been employed to prepare colloidal arrays. The structural templates used in generating periodic plasmonic nanostructures can also be fabricated in three-dimensional and two-dimensional colloidal arrays by self-assembly (Jiang et al., 1999; Sun et al., 2000; Jorge et al., 2007; Jang et al., 2008; Sun et al., 2008; Linn et al., 2009; Liu K et al., 2010; Sicard et al., 2010; Subbiah et al., 2010; Klang et al., 2012; Solans and Sol, 2012; Xu et al., 2012; Skorb and Moehwald, 2014; Johnson et al., 2015; Schmidt et al., 2015; Schwaminger et al., 2015; Siglreitmeier et al., 2015; Skorb and Andreeva, 2015; Yallappa et al., 2015; Yang et al., 2015). However, close-packed (CP) crystal structures have been prepared through traditional colloidal self-assembly, which is a low-throughput method incompatible with mature microfabrication. Obtaining non-CP (NCP) crystals allows the fabrication of more favorable photonic crystals with broad photonic band gaps (Hussain et al., 2014). Various functional plasmonic nanostructures such as coated nanoholes, metalized nanoarray surfaces, and polypeptide nanoparticles are able to demonstrate functional activities such as tumor targeting, active sensing, diagnosis, and drug delivery (Kralchevsky et al., 1994; Kim et al., 2009; Ahmad et al., 2010; Kereselidze et al., 2012; Kim, 2012; Koynov and Butt, 2012; Ding et al., 2014; Krpetic et al., 2014). However, this type of fabrication limits the yield and assembly of functional optoelectronic devices. We look at the current advancements of these encouraging techniques in synthesizing colloidals and their modifications with biomolecules, as well as their diagnostic properties. In addition to these advanced lithographic techniques, top-down techniques generally require very expensive instrumentations. These systems owe their immense sensitivity to the integration of precision processes, such as nanoimprint lithography (Yang H et al., 2013) and soft lithography (Zhang et al., 2015), with promising high-throughput patterns. There are methods using these kinds of techniques achieving sub-100-nm dimensions. Nevertheless, stripping difficulties related to master molds are still not solved because of high surface area on the nanostructures.

Many studies have been conducted to find an alternative lithography method based on adding blocks that organize themselves at higher or lower energy levels. Typical adding blocks are colloidal dispersions comprising colloidal particles diffused in a liquid medium. Recent advances for colloidal particles have enabled the synthesis of highly monodispersed colloidal particles with biomolecules to obtain more functional hybrid nanoscale materials. To utilize the unique properties of nanomaterials, these advanced methods have always been examined for a biological setting (Hayward et al., 2000; Joannopoulos et al., 2011; Im et al., 2011; Hasany et al., 2013; Han et al., 2014; Hashemizadeh and Huyeh, 2014; Hassan and Singh, 2014; Kumar et al., 2014; Gui et al., 2015; Guisbiers et al., 2015; Harris et al., 2015; Rodio et al., 2016).

Here, we have focused on biocolloidals, nanoparticles assembled with biological affinity tags that have been a popular object of study for the last 5 years. Considering the rate of development of new biohybrid particles, it is almost impossible to include them all in this review. However, we tried to choose the most exemplary ones, as highlighted in the Table and Figures 1–11. The list shows the broad applications of biocolloidals, such that the synergistic effect of the biological tags and the nanoparticles increase their functionality compared to when they are used alone. Thus, developing biocolloidals with enhanced properties and multimodality (simultaneous therapy, diagnosis, and theranostics ability) eases many biomedical applications, so they have easily become the center of interest for the researchers working at the interface of the bio-nano field.

2. Background: nanobiocolloidals

Fabrication of NPs can vary according to their core/shell structures or core/(shell)n structures, as seen in Figure 1 (Sapsford et al., 2011). In biological applications, the shell structures of NPs are usually designed to protect the inner layers. Most metal-, semiconductor-, and carbon-based NPs are hydrophobic, but they can become biocompatible through chemical modification of their surfaces with hydrophilic ligands. Besides avoiding the agglomeration of these particles in aqueous solutions, these hydrophilic ligands also increase the diffusivity of

Table. Representative biocolloidals' applications.

Nanocolloids	Biological tags	Advantage	Disadvantage	Application	**Ref.**
Metals	DNA proteins / enzymes carbohydrate / peptide lipid / DNA enzyme protein antibodies	Long-term effect, heat resistance, high efficiency	Oxidation (not for nobles), color change, blood clotting	Diagnostics energy harvesting / bioelectronics cellular labeling gene therapy / DNA delivery to cells sensing biocatalysis	Kralchevsky et al., 1994; Knoblauch et al., 2014
Semiconductors			Cytotoxic	Alzheimer's detection cell surface detection sensors / probes / cellular delivery	Yasun et al., 2013; Knoblauch et al., 2014; Verderio et al., 2014
Oxides	Peptides DNA / siRNA DNA / drug antibody / DNA	High efficiency, more stable, heat resistance	Membrane damage, poorly soluble	MRI imaging / sample concentration / therapy gene therapy drug and gene delivery bioanalysis / bioprobes	Yasun et al., 2013; Gui et al., 2015; Madden et al., 2015; Mahyad et al., 2015
Coated metals/oxides	Virus DNA	Biocompatible (for shells), noncytotoxic, synthesis in different forms	Poorly soluble	Bioelectronics / molecular memory subcellular organelle targeting	Herold et al., 2012; Zhu et al., 2015
Doped metal/oxides	Protein DNA	High efficiency	Dissociate into toxic materials	Biocatalysis bioanalytical probe	Hvastkovs et al., 2012
Polymers	DNA drug	Biocompatible, flexible, small, long-term effect, stable	Clotting, hemolysis	Optically coded hybridization probe imaging and delivery	Matea et al., 2015; Li et al., 2016; Zhao et al., 2016

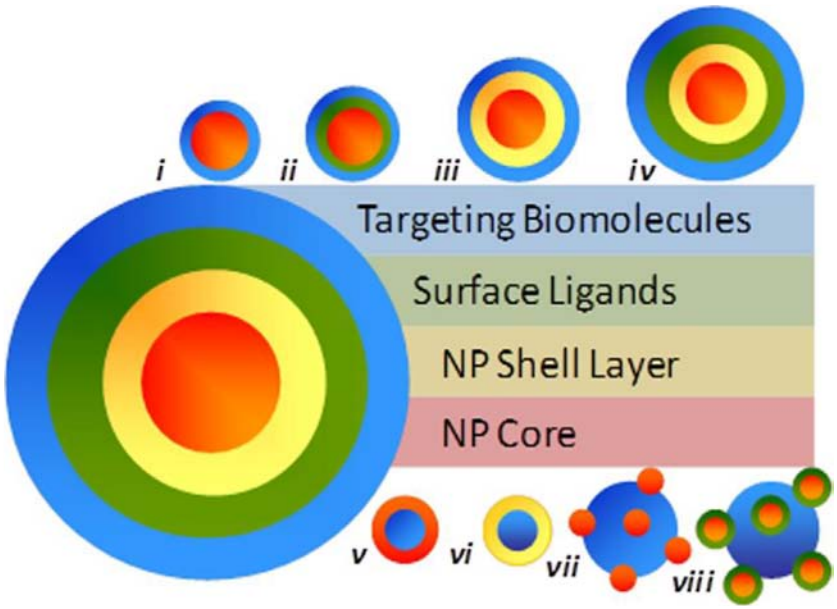

Figure 1. Some potential NP–bioconjugate components and multilayer bodies (not to scale): i) biomolecule connecting with NP center; ii) biomolecule connecting with a NP center via interface ligands; iii) biomolecule connecting with NP shell layer that covers the NP center; iv) biomolecule connecting with NP mid shell via interface ligands; v) porous NP center involving capsulated biomolecules; vi) spongy NP center involving capsulated biomolecules covered by a NP shell layer; vii) NP center (or NP center/NP shell bodies) particles are smaller than the biomolecule; viii) NP center (or NP center/NP shell bodies) particles are smaller than the biomolecule connected via interface ligands. Reprinted (adapted) with permission from Sapsford et al. (2011). Copyright 2011 American Chemical Society.

these particles and thus their retention times in biological media. After the particles are stabilized in aqueous solutions, the next step for generating biocolloidals is to attach bioaffinity tags (Table) to their surface for specific recognition of the biological target of interest. These tags can either be directly attached to the surface of the nanoparticles or they can be conjugated to the stabilizing ligands on the surface of NPs. The commonly known and employed bioaffinity tags that are responsible for biorecognition are antibodies, aptamers, enzymes, and DNAzymes. The multilayer structure of biocolloidals can be modified by several possible variations of core/shell/ligand/biomolecules (Stachowski et al., 2014). Figure 1 (Sapsford et al., 2011) shows eight schematic variations of NP-biological structures. The interaction of biomolecules with the NP core can happen in two ways: NPs can

either be surrounded by or encapsulate biomolecules (Stachowski et al., 2014). The variety of NP materials is broad and their dimensions can be adjusted between 100 nm and 1 μm. That is an important fact to consider for interactions between the biomolecules and NPs, since the sizes of large proteins can cause obstacles. However, NPs are usually larger than most biomolecules. Another obstacle can be the heterogeneity or polydispersity across a given population of the nanoparticles. Thus, fabrication methods for monodisperse particles are quite important for the success of the biological applications. As their sizes vary, NPs also have a broad surface area and volume range as well as relevant surface area : volume (S/V) ratios (such as sphere NPs with 100 nm to 1 μm diameters, volumes of 0.5 aL to 0.5 fL, surface areas of 0.03 μm^2 to 3×10 μm^2, and S/V ratios varying between 0.06 and 6 nm^{-1}). NPs cannot be dispersed until they reach small enough dimensions to be functionalized for colloidal dispersibility. On the other hand, NP surfaces do not usually have uniformity and are not very convenient for chemical modifications (Mahyad et al., 2015). Thus, most conjugation (hybridization) reactions on NP surfaces are not completely homogeneous. The self-assembly of the ligands on the surface of NPs is polydispersed across a population of NPs unless a strategic method is used, even if the NPs are homogeneously dispersed and diluted. These modification reactions can thus be achieved between the NP active sites and biomolecules (Joannopoulos et al., 2011; Cheng et al., 2011; Im et al., 2011; Mkenzie et al., 2012; Yang D et al., 2013; Kumar et al., 2014; Milionis et al., 2014; Prorok et al., 2014; Kang et al., 2015; Garrido et al., 2016; Mishra et al., 2016; Rodio et al., 2016).

The solvent-exposed residues also provide many active potential sites that are useful for intended labeling and solubility. The current modification methods of the NP biohybrids are still heavily inspired by the labeling methods for proteins. Molecular markers are generally produced on major scales as reactive dyes in fluorescent labeling. It is an efficient way, as the dye couples with multiple sites on the protein. Protein complexity is at a minimum because the dye molecules are generally larger than amino acid molecules. The reaction activity for labeling can be obtained experimentally, and the reactions can be adjusted empirically (Holtz and Asher, 1997). As their significant size holds various close target groups on the surface, the same approach is not considered feasible for biofunctionalization of NPs. The physicochemical properties of colloids hybridized with biomolecules are profoundly affected by the binding of multiple molecules at adjacent sites. Overactivation of the surface groups can result in less stability and colloidal accumulation. Multiple options based on size and surface area of NPs also contribute to the polydispersity for hybridization. The reaction stoichiometry usually does not depend on the NP biohybrid binding sites because hybrid reactions may not be well controlled (Stachowski et al., 2014; Mahyad et al., 2015). Thus, usually excess amounts of the biomolecules are employed in hybridization reactions, but these excess biomolecules should be isolated from the conjugates for the success of the intended biological application (Stachowski et al., 2014). Moreover, protein cross-links can be an alternative to NP–protein hybridization. On the other hand, this can provide NP–NP cross-linking depending upon the chemistry in technological applications. The proteins on NP surfaces generally contain functional groups, such as carboxyls and amines, that are accessible for hybridizations. Having a huge number of functional groups, NP–protein hybrids have more surface modification options. In contrast, artificial oligonucleotides and peptides may tend to be less reactive due to a lack of more functional groups. However, the flexible structures of biosynthetic molecules give them an opportunity to accomplish complicated, but adjustable, conformations.

3. Bioconjugated nanocolloidal particles

3.1. Metals

3.1.1. Gold and silver

The common features of the noble metals are chemical stability and resistance to oxidation. These metals are rhodium, palladium, silver, osmium, iridium, rhenium, ruthenium, platinum, and gold. Only palladium (Pd), platinum (Pt), silver (Ag), and most prominent noble metal among them all, gold (Au), will be examined in this section. A localized surface plasmon resonance (LSPR) occurs on the surface of plasmonic NPs by the excitation of the valence band electrons triggered by the interaction with the incident resonant light at a particular wavelength (SPR band), as represented in Figure 2 (Unser et al., 2015).

The wavelength (or frequency) of the SPR band or, in other words, absorption maximum, directly depends on the size and shape of the nanostructures and is also related to the refractive properties of the NP's environment. Spherical AuNPs are generally determined by a purple or a sharp red color and have a maximum absorption between 517 and 575 nm for particle sizes under 100 nm (Milionis et al., 2014). However, particles smaller than 2 nm do not include an LSPR band. The LSPR band is very sensitive to changes in size for nonsymmetrical NP surfaces, but the resonance band from spherical AuNPs shows weak size dependence. Rod-shaped AuNPs, known as "gold nanorods", show two LSPR bands that are defined as transverse and longitudinal bands. The transverse band is in the visible range of the spectrum, which is similar to that of a spherical AuNP, and longitudinal oscillation is in the NIR range of the spectrum (Herold et al., 2012; Yasun

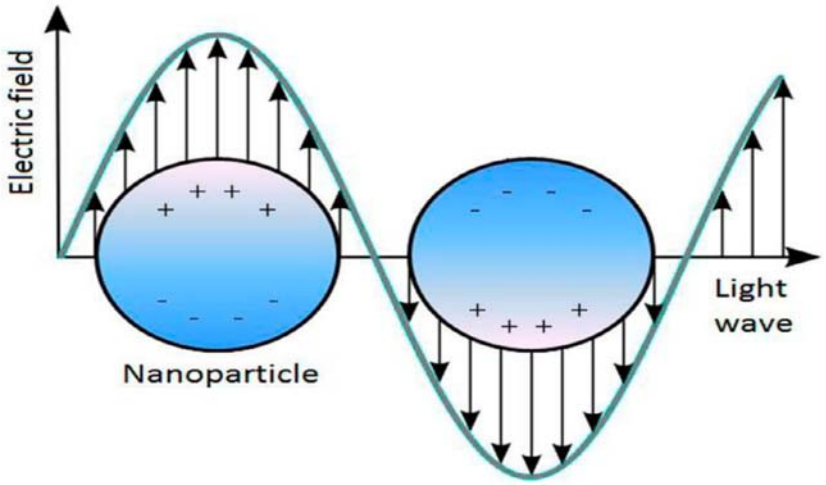

Figure 2. Schematic diagram illustrating the localized surface plasmon on a NP surface. The surface of plasmonic metal oscillated with incoming light generates radiating surface plasmons on metal NP surface. Reprinted (adapted) with permission from Unser et al. (2015). Copyright 2015 MDPI (Multidisciplinary Digital Publishing Institute), which is an academic open-access publisher.

et al., 2012, 2013; Kang et al., 2015). The longitudinal band shifts to longer wavelengths (red shift) and shows stronger intensities when the aspect ratio increases. There are various nanoparticles showing different morphologies, like polyhedra, plates, and hollow "nanoshell" shapes. They all have their unique and useful optical properties. These various shape choices can provide a strong LSPR that depends on shell thickness and the metal type. Among the other metal NPs, AuNPs are the ones most commonly used. AuNPs have useful catalytic effects. Moreover, for many bioapplications, the optical properties of AuNPs have also been found to be useful. In those bioapplications, the sensitivity of the LSPR to changes in AuNP size, shape, and surface is exploited. The wavelength shifts of the resonance band or visible wavelength changes can be used as analytical diagnostic tools. This property is demonstrated with the following use of gold nanospheres for very sensitive DNA detection (Kralchevsky et al., 1994). However, this procedure has also been used for the colorimetric detection of other bioanalytes, such as aptamers, oligonucleotides, and proteins. Au particles also provide efficient fluorescence switching, which has been used for developing probes and sensors that produce "on/off" signaling. AuNPs also provide beneficial potential applications in surface-enhanced Raman spectroscopy (SERS)-based assays because of the enhancement of the local electric field supported by the LSPR. However, AgNPs are usually preferred over AuNPs due to their contribution to the enhancements of SERS signals. These signals are better due to the intense electric field. Moreover, AuNPs that are almost 100 nm in size can efficiently show signals in dark-field microscopy via scattering and do this even better than fluorescence microscopy utilized in imaging processes (Klang et al., 2012). Most intensive absorption signals are obtained by AuNPs ranging between 10 and 50 nm in size. For photothermal therapy applications, absorbed light energy in the NIR range of Au nanoarrays such as nanorods and nanoshells is exploited (Herold et al., 2012; Yasun et al., 2013). Similar to AuNPs, AgNPs show a strong LSPR where the band is sharper and in shorter wavelength ranges (visible). Thus, they are higher in energy than Au nanoparticles (400–525 nm for dimensions 10–100 nm). AgNPs are therefore usually accepted to be superior materials for SERS applications (McBride et al., 2006), and they demonstrate higher enhancements compared to Au, Cu, and other metal particles. Additionally, Ag nanoparticles also provide potent antimicrobial properties and are used as antimicrobial and antiseptic agents. However, their shorter shelf-life and susceptibility to oxidation could diminish their impact in some applications (Yallappa et al., 2013).

A method to synthesize the AgNP–IgG–CF bionanocomposite silver is presented in Figure 3 (Matea et al., 2015). First, metallic silver (Ag^0) was obtained from reduction of silver ions (Ag^+) by sodium citrate. Immunoglobulin G (IgG) molecules were attached to calcium folinate (CF) molecules by covalent bonds in the second step. In the third step, silver nanoparticles were modified by the IgG–CF conjugation. To modify AgNP–IgG–CF nanocolloids and to prevent agglomeration, the suspensions were stored at ambient temperature 20 °C and 4 °C (Mullen and Banaszak Holl, 2011).

3.1.2. Palladium and platinum NPs

To obtain a biohybrid NP, biological substrates can also be utilized for templating PtNP synthesis. Examples of templating/stabilizing biomolecules can include graphene

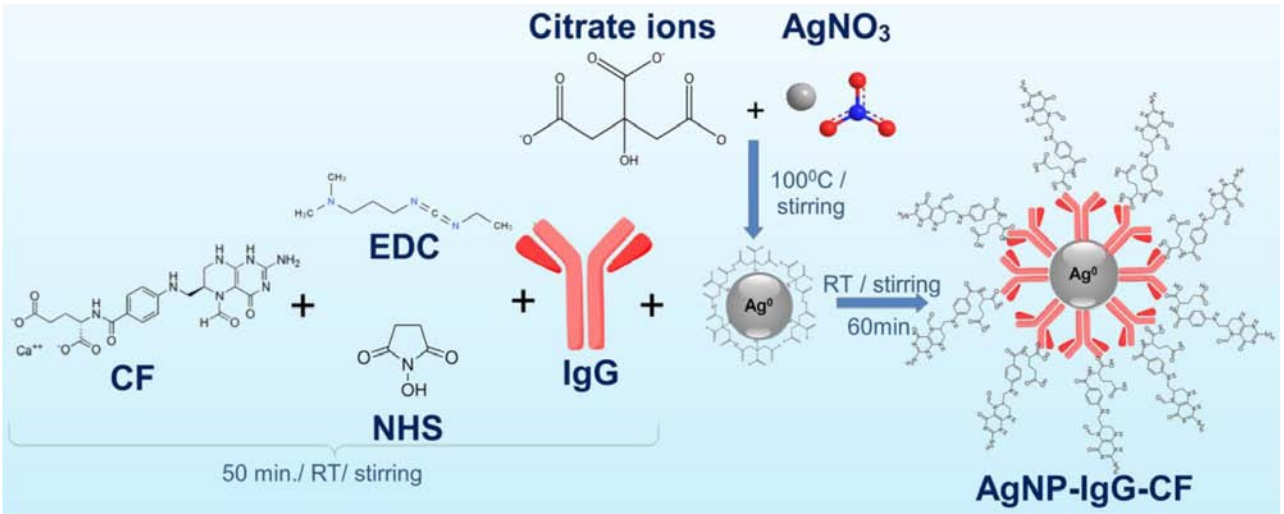

Figure 3. The synthesis protocol used for obtaining the AgNP–IgG–CF bionanocomposite is presented. Reprinted (adapted) with permission from Matea et al. (2015). Copyright 2015 Springer.

oxides (Devetter et al., 2015), bovine serum albumin (Giorgetti et al., 2012), and peptide bonds keeping different shapes of PtNPs between 2 and 8 nm in size (Vazquez-Gonzalez and Carrillo-Carrion, 2014). These proteins can also block the undesired toxic effects of the templating agents in biomedical applications (Khiyami et al., 2014; Yasun et al., 2015).

Dopamine has also been exploited for synthesizing PtNPs modified with the antibodies, producing a PtNP–poly(dopamine)–antibody composite (Vazquez-Gonzalez and Carrillo-Carrion, 2014). Conjugation of additional antibodies was achieved after adhesion or hybridization of a glutaraldehyde cross-linker to the surface. A spherical apoferritin cage has also been used to template PtNPs of 8 nm in diameter, so that biohybrids can show more cellular activity compared to the PVP-stabilized PtNPs (Vazquez-Gonzalez and Carrillo-Carrion, 2014).

3.1.3. Semiconductor quantum dots

Quantum dots (QDs) are nanocrystalline particles having an intrinsic luminescence feature. QDs are usually synthesized by doping III–V or II–VI group elements to form semiconductor alloys such as ZnS, ZnSe, CdS, CdSe, CdTe, or InP. Being considerably smaller than other plasmonic nanoparticles gives QDs unique photonic and electronic properties. However, since they are larger than the conventional organic dye molecules and protein markers that are used as biotags, they were initially considered to only be applicable to electronics. As the optical properties of QDs showed more functionality and larger quantum yields (QYs) compared to the conventionally employed fluorophores, they became the center of interest in tagging the biological molecules.

In bioapplications, the broad absorption profiles overlap with the photophysical properties that continuously work against the UV, narrow, size-direct proportional, and symmetric photoluminescence spectra scattering in wavelengths. They are fairly robust against chemical abrasion. Other important features of QDs include, but are not limited to, significant photostability (as QYs show), a substantial active Stokes shift, and the highest known multiphoton action (Velev et al., 1998).

Both center-only and center/shell-based QDs aim to protect the large energy band gap for improving fluorescent properties. On the other hand, passivating the core and preventing leaching are the two main fabrication methods for QDs to increase QY and decrease their toxic effects. Center/shell/shell QDs, center/alloy/shell QDs, and some other structural possibilities are also being currently used in biological applications. Here, we have predominantly focused on Se and Te alloys of Cd core or core/shell QDs, since they are widely employed in recent biological applications, while research for near-IR emitting features for other examples of QDs, including type III–V InP or InAs/ZnCdS, is still ongoing (Velev et al., 1998; Vickreva et al., 2000; Verderio et al., 2014). Monodispersed QDs have been synthesized in high quality by the reduction of organometallics with nonpolar coordination ligands in organic media. Following synthesis, the hydrophobic surface of QDs was functionalized with hydrophilic ligands to gain hydrophilicity to be dispersed well and to demonstrate their features in aqueous solutions.

QDs are commercially available from different vendors, but many research groups still choose to produce their own QDs and functionalize their surfaces by biotin,

amines, carboxyls, avidin, and oligonucleotides to generate biohybrid particles for their desired biological application.

When the synthesis routes of the QDs are examined in detail, there are two main strategies adopted for the fabrication of QDs. The first is the exchange of the two functional group ligands, driven by mass action, that binds the QDs at one site, generally by using thiol bonds, giving high solubility feature. The other is coating QDs with amphiphilic block copolymers to encapsulate the hydrophobic surface and generate a hydrophilic outer layer (as seen in Figure 4) (Algar et al., 2011). Despite the polymer layer on the QD surface, the subsequent bioconjugations can, via cap exchange techniques, access the surface of the QDs. QD features are highly dependent on the chosen fabrication strategy. While the method applied for encapsulation yields larger sizes with higher QYs, the cap exchange typically results in lower QY and smaller QDs. When generating biohybridized QDs, it is significant to consider these factors because they can affect biological applications such as FRET interactions, cellular transports, diagnosis in vivo, and distribution (Velev et al., 1998; Vickreva et al., 2000; Knoblauch et al., 2014; Verderio et al., 2014).

The surface functionalization of QDs to obtain their biohybrids can be classified into six subgroups based upon the type of the attachment used or the variety of surface ligands that are tethered. These methods involve: 1) covalent attachment of the ligands and intended functional groups on QDs; 2) electrostatic attraction between excited QDs and oppositely charged biomolecules; 3) physical interactions among the inorganic surface of the QDs, thiol groups, and polyhistidine sequences of biomolecules; 4) noncovalent, high-affinity bindings, such as between streptavidin-pretreated QDs and biotin-labeled biomolecules; 5) enzyme-catalysis; and 6) templating via biosubstrates. Unfortunately, some of these approaches can cause uncontrolled mutlivalency on the surface of QDs, which result in undesirable cross-linking. For example, aptamers within one QD can bind to the same target biomolecule (i.e. a protein with more than one homogeneous binding site) and might decrease the signal intensity (Mayoral et al., 1997; Liu X et al., 2010; Lukianova-Hleb et al., 2012; Martinolich et al., 2012; Mkenzie et al., 2012; Monguzzi et al., 2014; Montano et al., 2014; Luo et al., 2015; Madden et al., 2015; Mahyad et al., 2015; Matea et al., 2015; Mishra et al., 2016).

Thus, the surface modification of QDs with the listed affinity tags and biomolecules (such as in proteins, peptides, DNAs carbohydrates, and drugs) allows the biohybrid to be employed in different biological applications, as shown in Figure 5 (Zrazhevskiy and Gao, 2013; Cutler et al., 2013).

3.2. Metal oxide NPs

3.2.1. Iron oxide

There are two main forms of iron oxides (IOs): magnetite (Fe_3O_4) and its oxidized form, maghemite (γ-Fe_2O_3). One of the widely employed types of nanomaterials with diameters between 1 and 100 nm are iron oxide NPs (IONPs). Much attention was drawn to their significant features, which make IONPs very suitable for potential technologic applications in materials engineering and biological sciences (Griesser et al., 2002; Harris, 2004; Fudouzi and Sawada, 2006; Gioux et al., 2010; Gabudean et al., 2012; Giorgetti et al., 2012; Frank et al., 2013; Garg et al., 2013; Gatto et al., 2013; Hasany et al., 2013; Ghosh and Collie, 2014; Gonella and Dai, 2014; Hashemizadeh and Huyeh, 2014; Hassan and Singh, 2014; Gui et al., 2015; Guisbiers et al., 2015; Harris et al., 2015; Helmbrecht et al., 2015; Garg, 2016). Since they are relatively nontoxic to human organs, magnetite and maghemite are selected to be used in biomedical applications. Iron oxides are partially biodegradable materials and therefore are practical for in vivo applications. One popular application of IONPs is high sensitivity biomolecular MRI for treatment and clinic diagnostics. However, this application requires IONPs to be coated with ligands such as diols, alkyl amines, and macro-chain fatty acids. In their therapeutic applications, reactive oxygen species with controlled local toxicity could destroy disease-causing tissue, with diminished side effects compared to conventional chemotherapy strategies. On the other hand, because of their remote controllability with an applied constant external magnetic field and their antitumor activity, hyperthermia below 40 °C can be complemented with drug loading, and this synergy could be more advantageous than conventional antitumor drugs.

The spin state of magnetic particles determines their reactivity. The relationship between the electromagnetic wavelength of radiation with magnetic properties and the paramagnetic cores of the complex was found via experimentation. Controlling the kinetics of radical systems by magnetic fields and altering the level of toxicity (oxidative stress) in a malignant tumor is possible. Since tumor tissues are undefended against oxidative stress and high levels of local toxicity in tumor area, these IO structures can prevent the growth of cancer cells. They can be designed as therapeutic agents that prevent abnormal growth of tumor cells. Also, the multifunctionality gained by biomolecule hybridization allows IONPs to be used in magnetic nanotherapy, tumor targeting, and medical imaging as theranostic applications for personalized treatments. If the sizes of ferromagnetic substrates are smaller than the size of magnetic domains, supermagnetism happens on the nanoscale (Ho et al., 1990; Heo et al., 2009; Herold et al., 2012; Hermanson, 2013; Helmbrecht et al., 2015). Superparamagnetism (SP) takes place in the

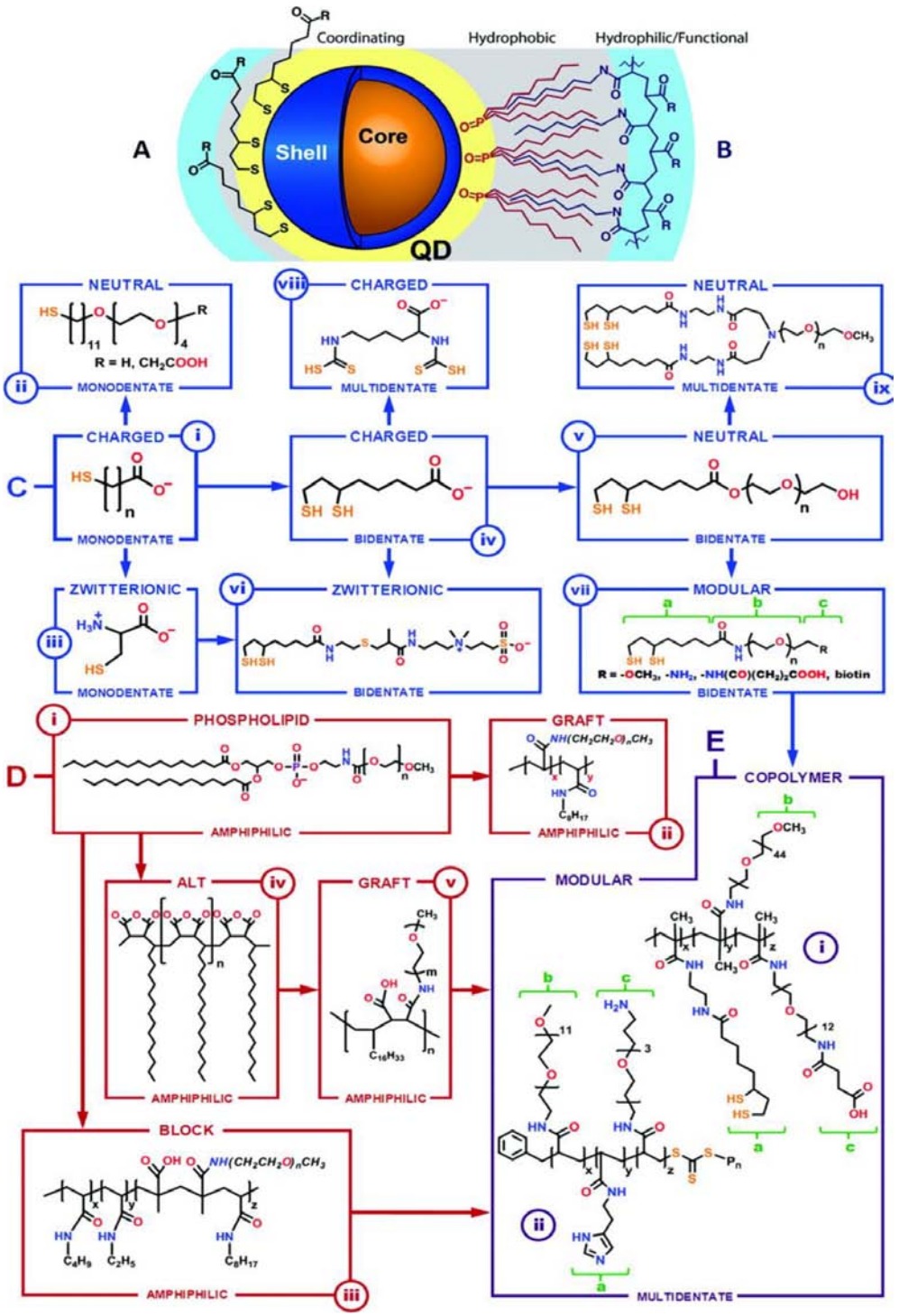

Figure 4. Schematic of the chemistry of core-shell QDs. (A) Ligand bindings at the QD surface are depicted. (B) Unification of a blue amphipol with the inorganic QD red ligands. (C) Ligand groups are given: i) thioalkyl acids, ii) PEGylated ligands, iii) zwitterionic ligands, iv) dihydrolipoic acid ligands and v) PEGylated, vi) zwitterionic, and vii) modular derivatives like viii) multidentate-charged and ix) multidentate PEGylated ligands. (D) The amphipol shells: i) phospholipid micelles, ii) hydrophilic polymer backbones modified with alkyl chains, iii) triblock copolymers, and iv) alternating copolymers that turn into acids or v) are modified with PEG chains. (E) Copolymers with pendant PEG oligomers and i) dithiol or ii) imidazole groups. Discrete moieties for (a) QD binding, (b) solubility, and (c) biological link points are green. The arrows are used for a conceptual progression instead of synthetic pathways and chronology. Reprinted (adapted) with permission from Algar et al. (2011). Copyright (2011) American Chemical Society.

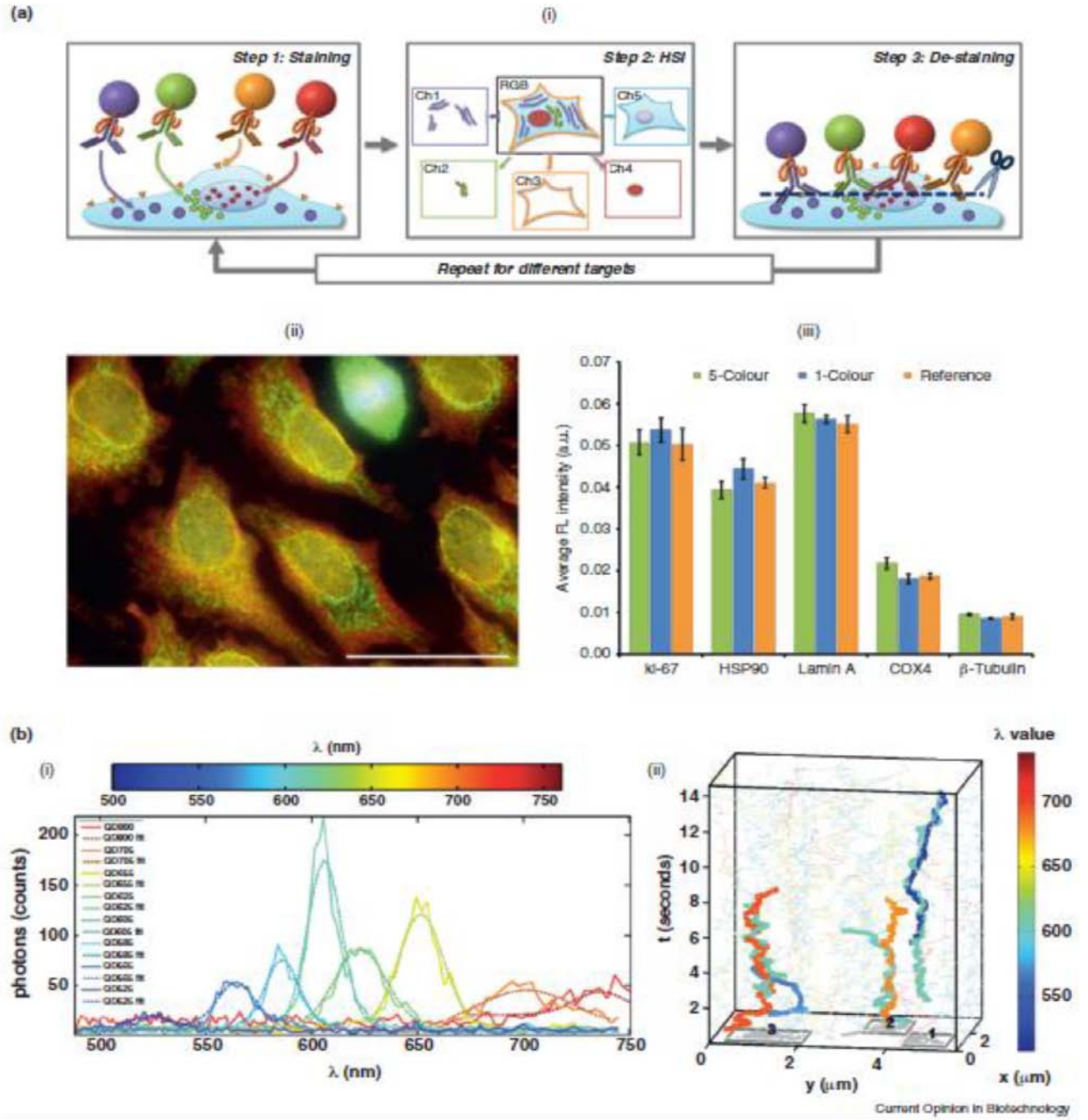

Figure 5. Current examples of multiple QDs. (a) Five different colors of QD provide immunostaining of cell surface biomarkers and hyperspectral imaging, with subsequent decoloring and recoloring: i) assay protocols; ii) symbolic 5-color image (scale bar = 50 mm); iii) approval of 5 different coloring. Reprinted (adapted) with permission from Zrazhevskiy and Gao (2013). Copyright 2013 Nature Publishing Group. (b) Hyperspectral SPT with QDs: i) single particle emission spectra for 8 colors of QD; ii) obtained trajectories for the different colors of single QDs. Reprinted (adapted) with permission from Cutler et al. (2013). Copyright 2013 the Creative Commons Attribution License.

single magnetic domain. The kinetic energy carried to the system from thermal vibration energy is enough to reverse magnetization. Therefore, SP materials indicating paramagnetic features can also show significant magnetic susceptibility. When placed into a magnetic field, their magnetic moments tend to align along the applied field, but they do not retain any net magnetization once the external magnetic field is eliminated. Biopolymers like

polysaccharides, including dextran and chitosan (CHI), are the most commonly used dispersants to modify the surfaces of SP materials to obtain stable colloidal solutions. The dimension and coating type of IONPs determine their biodistribution while labeling the tissues of interest (Holtz and Asher, 1997; Holland et al., 1998; Howes et al., 2014). Thus, IONPs are designed as MRI contrast agents. Recently, it was demonstrated that IONPs can be used as energy transporter agents for thermal therapy applications of cancer (Hussain et al., 2014) and other biomedical applications (Hvastkovs et al., 2012). The thermal therapy approach has already shown some clinical success where cancer cells were cauterized with temperatures above 46 °C. IONPs can be biocompatible after certain surface modifications. They are deactivated by the liver as an iron pool, and then they are totally removed in 2 days (Jang et al., 2008; Janib et al., 2010; Im et al., 2011; Baldassarre et al., 2015).

IONP synthesis is achieved by the most economic and widespread synthetic method, called the Massart method, where a defined stoichiometric ratio of Fe(II) and Fe(III) salts is precipitated in solution conditions to make γFe_2O_3 NPs (Hasany et al., 2013; Ferreira et al., 2016). This technique can be used to fabricate massive amounts of highly monodispersed population of IONPs. This crystal development employs a pretreated templating method where reverse micelles (Qiu et al., 2012), liposomes (Peretz and Regev, 2012), dendrimers (Jethmalani et al., 1997), phospholipid vesicles (Tekin et al., 2007), or apoferritin protein cages are used as confining agents (Kostiainen et al., 2013). The synthesis of monodispersed IONPs usually relies on certain arranged conditions of the reaction medium (pH, temperature, concentration, etc.). On the other hand, thermic degradation of organometallic Fe reactants offers a simple way to fabricate highly monodispersed and crystalline IONP particles (Hagenson and Doraiswamy, 1998; Lei et al., 2011; Jia et al., 2015; Lee et al., 2016). Thermal methods are generally achieved in organic solvents with high boiling points. There are also other methods available to fabricate IONPs than the ones explained here (Jang et al., 2008; Linn et al., 2009; Luo et al., 2015).

In general, biofunctionalization of IONPs can be achieved with either direct hybridization to the native oxide surface or indirect hybridization to the stabilization layer. One of the most important steps in the IONP fabrication process is to use surface stabilizers or ligands to prevent aggregation of colloids during the reaction process. These stabilizers might also be mixed via postfunctionalization methods with IONPs. There are various stabilizers utilized for IONP surfaces such as carboxylates, phosphates, polymers, and inorganic materials like silica and gold materials (Jang et al., 2008; Linn et al., 2009; Luo et al., 2015). Colloidal repulsion provided by the similar molecular layers can either be electrostatic (Kalsin et al., 2006) or steric (Adams et al., 1998) in nature. It is again necessary to emphasize that these coating shells have a significant role in intended biomodifications of the IONPs, so they have a dual beneficiary role for the surface modification of IONPs. The coatings and shells on IONP surfaces are generally exploited as the binding sites for chemical/biological functionalization since the IONP surfaces are usually inert and inaccessible.

3.2.2. Silicon dioxide

Although current attention mainly focuses on the fabrication techniques of metal colloidals, silica NPs (SiO_2 NPs) were one of the earliest artificial NP materials to be examined in detail (Pan et al., 2013). Because of their biocompatibility, large surface areas, and facile surface modifications, SiO_2 NPs have contributed to a wide range of biological applications such as drug delivery (Park and Hamad-Schifferli, 2010; Pereira et al., 2014) and diagnostics (Peretz and Regev, 2012). Encapsulation of fluorescent dyes is one of the most important roles of SiO_2 NPs for bioimaging purposes. Huge loads of fluorophore molecules can be encapsulated in SiO_2 particles to act as a superfluorescent NPs (Kainz et al., 2010; Pergantis et al., 2012; Tan et al., 2012; Zhu et al., 2014; Helmbrecht et al., 2015; Luo et al., 2015). On the other hand, this encapsulation is also applicable to NPs that are not biocompatible. SiO_2 layers can be polymerized on the surface of those toxic particles to form a shell to generate biocompatible hybrid NPs (Pokhrel et al., 2014; Pla-Roca et al., 2015; Del Mercato et al., 2016; Filip et al., 2016; Li et al., 2016; Piella et al., 2016). Fabrication techniques, such as hybrids, are actually quite hard to achieve by applying silane chemistry, but many SiO_2 NP biohybrids are still synthesized and employed due to their utility (Polavarapu et al., 2014).

The Stöber method is the most common synthetic route employed to fabricate SiO_2 nanoparticles. In this method, organic silanes, such as tetralkyl silyl esters, are hybridized with trace amounts of ammonia in an alcoholic solution (Prevo and Velev, 2004; Pan et al., 2013). The polymerization of –O–Si–O– silanes takes place in the presence of ammonia that acts as a capping agent, stabilizes nanoaggregation, and determines the dimension and morphology of the SiO_2 NPs. Even though many other methods are also available, most SiO_2 NPs are still exclusively fabricated using this procedure (Park et al., 2009; Ahmadivand, 2012; Ahmadivand et al., 2012; Vazquez-Gonzalez and Carrillo-Carrion, 2014; Wen et al., 2014).

There are several examples mentioned below regarding the spin coating technique based on the Stöber method. One of the colloidal templating approaches is

the fabrication of arrays of Au half-shells with preferential upright orientation, as shown in the schematic outlining the templating process in Figure 6 (Liu et al., 2010). Silica colloidal particles with unordered NCP structure prepared by the spin-coating technology are manipulated as a structural template in this method. The sharp edges of the upright-oriented half-shells and the small gaps between close shells might both work as electromagnetic "hot spots" to enhance the electromagnetic field to reach very high SERS enhancement factors (up to 10^{10}). Nagpal et al. proved that smooth-templated structures with optimum surface-plasmon-propagation length are critical for plasmonic composite chip devices and can be fabricated by patterning methods, since the anisotropic engraved silicon pyramidal pits are very smooth and homogeneous (well-oriented) (Yang H et al., 2013; Nomura, 2012; Liu et al., 2015). Also, reverse silicon pyramids can be utilized to pattern polymer pyramids instead of templating pure Au nanopyramid arrays (Lyshevski, 2005; Askar et al., 2013; Liu XF et al., 2013; Liu X et al., 2015). Metal films can coat polymer structures to fabricate functional plasmonic nanoarrays. The scanning electron microscope images show Au half-shells prepared with different thicknesses and upright-oriented: 30 nm thick (Figures 6A and 6B) and 70 nm thick (Figures 6C and 6D) (Liu et al., 2010). These sharp metal nanoshells have promising beneficiary roles for optics, data storage, and biosensor applications based on photonic materials having a curvature radius of less than 5 nm.

3.2.3. Titanium dioxide

Titanium dioxide NPs (TiO_2 NPs) have been used in a broad range of research fields, such as pigments (Im et al., 2005), optics (Haynes and Van Duyne, 2001; Chen X et al., 2008; Dou et al., 2012), sensors (Bhatia et al., 2013; Cennamo et al., 2013; Chung et al., 2013), and cosmetics (Im et al., 2005). Recently, as a significant photoactive ingredient, they have been employed to improve solar cells (Nel et al., 2009; Chen et al., 2012; Banerjee et al., 2015) and photocatalytic reactions (Sun et al., 2006; Manera et al., 2012; Xiao, 2012). However, their applications in the biomedical field are still underdeveloped due to concerns about their biosafety (Homola, 2006; Liu X et al., 2013), or in other words, due to their long-term toxic effects (Han et al., 2011; He et al., 2011). The photocatalytic effects of TiO_2 NPs are, however, exploited to improve bactericidal composites (Jokinen et al., 1998) and photoactivated cancer treatments (Rabarot et al., 2003; Banerjee et al., 2015). Moreover, TiO_2 NPs have physicochemical characteristics that can be simply utilized for sensor studies like photoelectrochemical sensors for gas detection (Homola, 2008; Howes et al., 2014). TiO_2 NPs can be fabricated by a variety of methods (Chen et al., 2011; Chen et al., 2012). In the commonly used sol–gel technique (Maduraiveeran and Ramaraj, 2013), some inorganic Ti reactants, like titanium tetraisopropoxide (a titanium alkoxide, $Ti(OR)_4$ (R = alkyl)), are chosen to lead the formation of Ti–O–Ti polymer chains. Nonhydrolytic synthesis (sol–gel technique) is another method of fabrication that uses

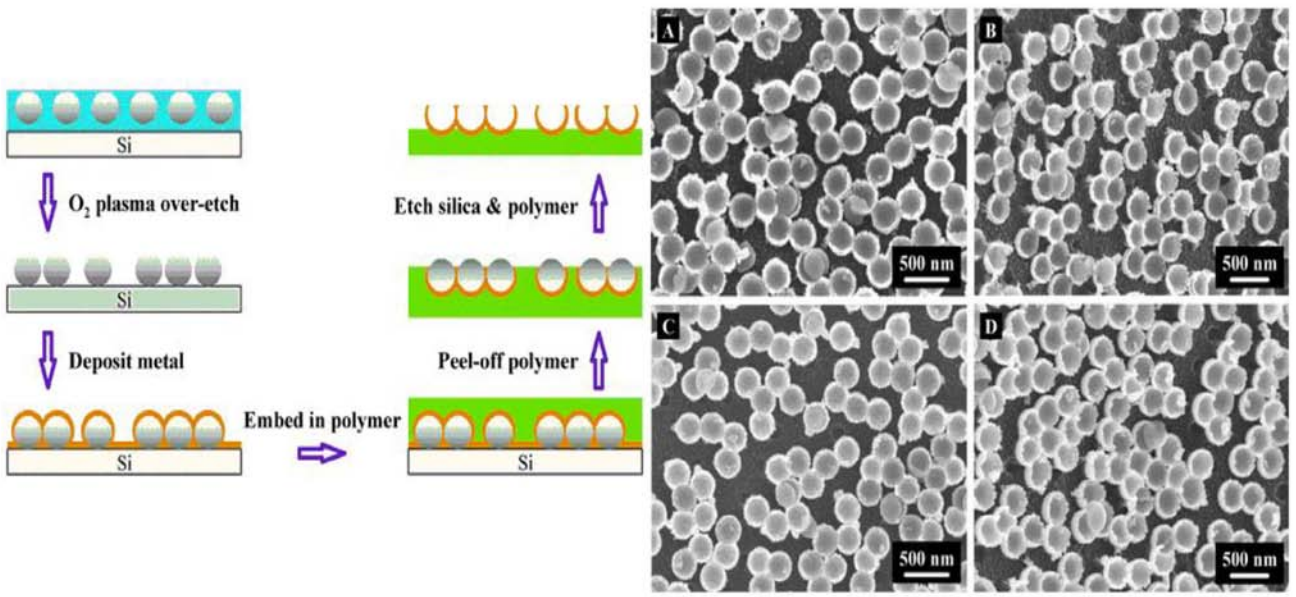

Figure 6. The templating procedures schematically given for fabricating metal half-shells upright-oriented by using randomly arranged silica colloidal monolayers. SEM images show Au half-shells prepared with different thicknesses and upright-oriented: (A and B) 30 nm. (C and D) 70 nm. All metal half-shells are obtained from 300 nm silica spheres. Reprinted (adapted) with permission from Liu et al. (2010). Copyright 2010 Royal Society of Chemistry.

capping agents (Kajihara and Yao, 2000). There are other less common synthetic routes, such as solvothermal, oxidation (De Azevedo et al., 2006), hydrothermal (Sun et al., 2005; Xing et al., 2015), chemical vapor deposition (Lee et al., 2007), physical vapor deposition (Johnson and Walsh, 2011), electrodeposition, sonochemical, and microwave-assisted synthesis to fabricate TiO_2 NPs (Chen TH et al., 2008; Yallappa et al., 2013; Ali et al., 2015; Amiri et al., 2015; Helmbrecht et al., 2015). The techniques used for the hybridization of biomolecules to their surfaces have been examined and partially summarized in reports (Pieranski, 1983). One simple way of modifying the surface is conjugation with silanes (Boulares-Pender et al., 2009; Zeira et al., 2009; Algar et al., 2011; Maduraiveeran and Ramaraj, 2013). This conjugation is typically carried out with strong donor ligands, but the Ti–O bond is still extremely powerful (He et al., 2011; Banerjee et al., 2015). For example, by using (3-aminopropyl)triethoxysilane in anhydrous dimethyl sulfoxide, TiO_2 NPs can be functionalized with amino groups (Vilela et al., 2014).

Generally, while changing their optical and catalytic properties, catechol ligand derivatives can form stable bonds on TiO_2 surface (Jokinen et al., 1998; Manera et al., 2012; Xiao, 2012; Park et al., 2013). These groups can then be used for further surface functionalizations with biomolecules. For example, TiO_2 NPs functionalized with dihydrophenylacetic acid can form amide bonds with biomolecules through EDC/NHS chemistry. Thus, this conjugate can be hybridized with antibodies to be employed in targeted photoactivated cytotoxicity applications for A172 and U87 brain cancer cell lines (Yokel et al., 2013). It has been proven that dopamine can also be a valid generic linker that can functionalize the surface of TiO_2 NPs with amines (Manera et al., 2013). For this purpose, dopamine was employed as a heterobifunctional linker for tethering the oligonucleotides and biotin to the surface of TiO_2 NPs (Yasun et al., 2012; Bong et al., 2015). TiO_2 NPs can form a durable complex with phosphates and phosphonates (Tien et al., 1997). This hybridization technique has been utilized for the interaction of Gd ligands for MRI probes (Susumu et al., 2007; Muller and Batchelli, 2013). Phosphonates and bisphosphonates can build covalent bonds with TiO_2 NPs in the form of the –P–O–Ti–O–P– coordination type, which provides high loading levels (Susumu et al., 2009).

3.3. Polymeric nanomaterials

Natural polymeric nanomaterials are biological substitutes for synthetic materials, and they are derived from polysaccharides, polynucleotides, oligonucleotides, proteins, or polypeptides (Arsenault et al., 2004).

Biopolymeric nanomaterials are fabricated with various methodologies such as evaporation of emulsion/solvent, solvent displacement, complex coacervation, and salting out to have a polymeric nanomaterial formation (Ruhl et al., 2003; Wang et al., 2008; Urban, 2014).

Moreover, ionic gels, opposite coulombic charges among polyelectrolytes, and basic self-assembly are different routes for their synthesis based on the electrostatic interactions and amphiphilic features (Linn et al., 2009; Lima-Tenorio et al., 2015). Immunogenicity and toxicity can be induced by the contents of the synthetic nanomaterials, but many biopolymer-based nanomaterials can be biodegradable and are generally considered to be minimally toxic compared to their artificial rivals. However, there are still challenges encountered during their fabrication, such as purity of biopolymers and batch-to-batch reproducibility. Biopolymeric nanomaterials obtained from natural polymers, such as polycarbonates and primary and secondary proteins, have been exploited in various medical applications, such as therapeutic delivery and bioimaging (Lee et al., 2004; Li Y et al., 2011; Li et al., 2013; Li et al., 2016). They can embody various functional moieties for biomodification with natural biosubstrates. As examples, internal and external photoluminescent labeling, cross-bonding, physical adsorption, mutagenesis, and genetic unification can be given. Multifunctional nanomaterials are designed to increase the efficiency of the final complex to be used in bioapplications. Biopolymers are convenient candidates for the fabrication of multifunctional nanomaterials with their highly modifiable various functional moieties. Therefore, briefly, these structures will be examined throughout the following sections. Only representative examples and the features of the corresponding polymers (Figure 7 (Massey et al., 2015)) are chosen here for illustrative purposes within this vast field.

3.3.1. Polysaccharides

Polysaccharide molecules are composed of repeating mono- or disaccharide monomers that are linear, branched, and even cyclic in nature. Since a number of these biomolecules have previously been applied in micrometer sizes, they are primarily known as NPs. CHI is the most common polysaccharide nanomaterial functionalized with biosubstrates (involving drug molecules) for biomedical applications such as gene delivery and for oral and ocular therapeutics (Lyshevski, 2005; Lynch et al., 2007; Lukianova-Hleb et al., 2012; Fen and Yunus, 2013; Luo et al., 2015; Mansur et al., 2015; Luo et al., 2016). Besides facilitating the electrostatic self-assembly of DNA because of their highly cationic nature, CHI molecules are highly popular due to their primary amines that form the polymer backbone. Other polysaccharides have been accepted as NPs, although their potential hybrid sites have more restriction than CHI. Alginate (ALG) is generally prepared as caps, bowls, beads, and microspheres for biomedical applications, (Shim et al., 1999), except for its hybridization with CHI. However, ALG is weakly accepted as a nanomaterial. Biological cellulose and starch

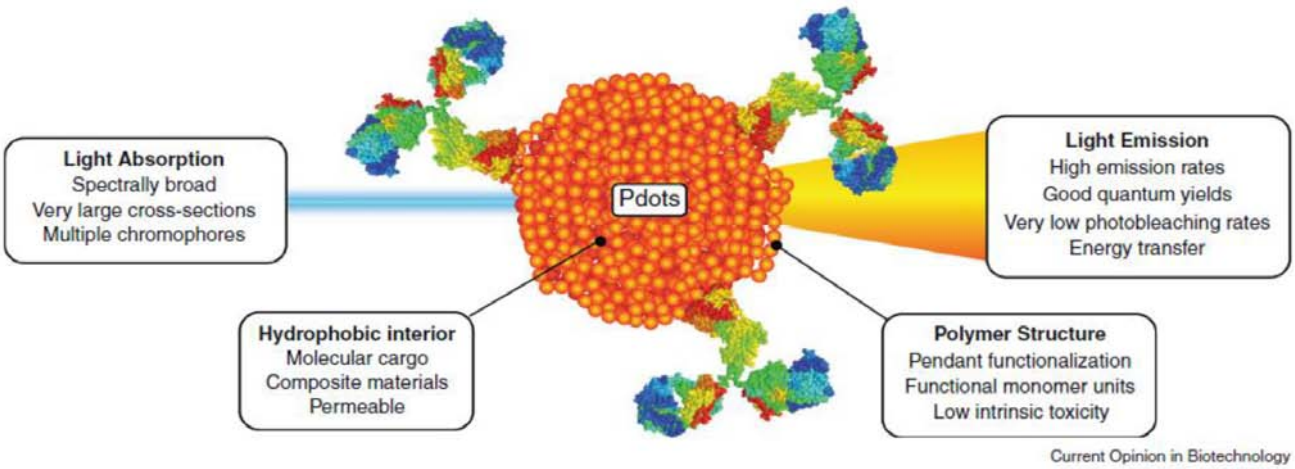

Figure 7. Advantageous properties and features of Pdots. Reprinted (adapted) with permission from Massey et al. (2015). Copyright 2015 Elsevier.

molecules are the most commonly known carbon-based polymer sources. Starch NPs (Milionis et al., 2014) and cellulose nanocrystals (Zhang et al., 1999; Bhattacharya et al., 2010) have usually been employed as biohybrids in the potential applications of molecular visualization and biosensors. One of the most commonly used polysaccharide materials is hyaluronan (HAA), known as hyaluronic acid. HAA, similar to ALG, has been utilized as microspheres for drug delivery applications. However, it is currently being functionalized as a NP (Mansur et al., 2015). Since it was proven that tumor cells excessively express some HAA receptors, HAA nanomaterials have attracted significant attention for being natural probes (Bowers et al., 2005; Martinolich et al., 2012; Matea et al., 2015). Also, polysaccharides generally embody active groups consisting of amines, hydroxides, and carboxylic acids that might be used for biohybridizations; however, capsulation is the most commonly used technique for hybrid biomolecules to date.

3.3.2. Proteins and polypeptides

Various protein-based particles have previously been prepared in microns with polysaccharide-based nanomaterials. Gelatin, as the most common derivative of collagen, and albumin, as the most abundant protein in plasma, can form materials and be obtained from harvested precursors, but self-assembled polypeptide structures are a broad and more utilized class of materials. For example, specific protein molecules and peptide structures, tertiary protein molecules (Jang and Kim, 2011; De Backer et al., 2015) (integrated with surfactants), casein (Tielemans et al., 2006; Qiu et al., 2012; Seisenbaeva et al., 2012; Yasun et al., 2015), various ionic structures, or two-faced peptides (Breitling et al., 2009; Coppage et al., 2012; Knez et al., 2013) will form self-assembled nanoscale structures in laboratory conditions (Newcomb et al., 2012). Protein cages offer different interior and exterior functional regions that can be utilized for different modifications and are one of the polypeptide-based materials that are increasingly being offered for bioapplications (Bhattacharya and Mukherjee, 2008; Mukherjee et al., 2014; Devetter et al., 2015; Kumar et al., 2015). Other commonly known protein structures involve heat shock proteins, ferritin, and viral-coat materials. Ferritin and viral-coat materials are explained in the current sections. Owing to their biocompatibility, biosafety, biodegradability, and general low toxicity, protein-based nanomaterials have attracted significant interest in drug delivery applications (Nomura, 2012; Nygaard et al., 2012; Nishiguchi et al., 2015). Thus, chemical and affinity tag functionalization of those protein-based materials can open new directions in targeted therapeutics and bioimaging with negligible cytotoxicity.

3.3.3. Synthetic polymer NPs

The popular and complex areas of polymeric nanomaterials cover both classical polymeric substrates and dendritic-type structures. The subject of a number of current reviews is the impulsion force behind employment of these nanoparticles in drug and gene delivery (Baffa et al., 2009; Bartel, 2009; Matea et al., 2015; Cheng et al., 2016). Generally, while recently decreasing their toxicity through reduction of the necessary dose, the NPs employed for drug delivery should be dispersible, robust, and have reasonable retention times.

Even though multifunctionality is not unique to polymer-based NPs, their polymerization can offer a broad range of different structures as well as different functional moieties because they can be synthesized with various isomers and monomers (Zhao et al., 2016).

On the other hand, polymer-based NPs can be used in sensor platforms due to their physical or chemical changes in response to a stimulus, which can then be utilized as a signal transduction. For example, these stimuli can be the changes in environmental temperature, pH, and enzyme activity. On the other hand, these stimuli-induced changes or the responsive nature of the polymer-based NPs can be exploited in controlled therapeutic applications such as drug delivery and release. Usually, polymer-based NPs include a benefit over lipid systems, as they can be prepared to be chemically durable even in dilute solutions. NP structures specifically provide advanced biomolecules delivery abilities, comprehensive insulation from the physical environment, and more capabilities over drug delivery while non-cross-polymer net structures have been exploited to transfer drug and gene molecules (Xiao et al., 2015).

3.3.3.1. Classic polymer NPs

As recently reviewed (Baxter et al., 1997; Brands et al., 2005; Chen et al., 2005; Chen et al., 2006; Budkowski et al., 2009; Samusev et al., 2011; Aime and Coradin, 2012; Budkowski et al., 2012; Gui et al., 2015; Xiao et al., 2015), classic polymer NPs can be fabricated by using a fixed ratio of monomer and initiator for both hydrophobic and hydrophilic surfaces by utilizing different techniques. For example, polyglycolic acid, polylactic acid, and polylactic-co-glycolic acid (PLGA), hydrophobic functional groups, are synthesized from polyesters. One of the common materials also involves polyvinyl chloride and polystyrene (PS). Attaching carboxylic acid groups to their bulk surfaces develops hydrogen interaction and improves polarity of solutions, especially at low MW.

PLGA, along with a few other corresponding systems, is already used in some biomedical devices approved by the US FDA. The common hydrophilic substrates for nanomaterials involve polylysine, polyethyleneimine, poly(amidoamine), poly(N-isopropylacrylamide), poly(alkyl cyanoacrylate), polyethylene glycol, and poly(methyl methacrylate). Polymeric nanobowls, nanocrescents (Liu et al., 2013), and nanofibers have also been fabricated and have many technological applications in biodiagnostics, while polymer nanosystems have been receiving considerable interest so far (Dziubakiewicz et al., 2013; Elsabahy and Wooley, 2013; Farkhani and Valizadeh, 2014). The abundance of monomers and polymer initiators is one of the most important advantages that contribute to polymeric NP development.

3.4. Hybrid NP materials

Composite NPs consisting of many systems are fabricated or built with at least two or more different materials. The composite NPs are distinct NPs that demonstrate unique features of the NPs that form them. Because of the variety of these materials and distinct chemical materials used for their biohybridization (albeit generally similar to those already explained herein), this topic is out of the scope of this review. Recently reviewed prototypical examples of these NPs are here for illustration. Many nanomaterials are designed to have particular, significant properties that would not exist within composite systems built from a single material.

Group II–IV semiconductor nanocrystals are designed as center/shell structures: for example, CdSe/ZnS, CdSeS/ZnS, and CdTe/ZnS. These systems involve two or more distinct structures prominent in biological uses (Dalton et al., 1999; Jiang, 2001; Nitta and Steiner, 2005a, 2005b; Gatto et al., 2013; Jia et al., 2015; Zhao et al., 2016). Semiconductors have significant hybrid materials for point of control diagnosis techniques that exploit large fabricated consumer devices that are preferred to bulky scientific instrumentation. As seen in Figure 8 (Petryayeva et al., 2014), quantitative and laminated FRET-based structures are shown with economic UV visible light sources as an illustrative example (Lyshevski, 2005; Gadegaard et al., 2006; Montano et al., 2014). Here, the QD structures allow detection of the broad and strong absorption ranges by utilization of a visible LED light for stimulation, which is acquired by the built-in visible color filters of the smartphone camera without noise. Their direct application to this field provides lower absorption and wider emission from fluorescent molecules.

An approach designed by Spillmann et al. has been to improve self-assembled polymeric liquid crystals to keep the interactions of a fluorescent hybrid molecule for the NP under control (Zhu et al., 2014). To determine vinyl functional ends attached to the ends of functional groups of the molecule and integrated with colloids, a perylene derivative (PERC11) was prepared by a solution, including emulsion, then completed by thermal polymerization. The synthesized NPs, with diameters between 50 nm and 300 nm, were then centrifuged to receive a sample showing <10% polydispersity, and then these were size-selected. More significantly, the obtained emission spectrums could be examined by monitoring the aggregation of the perylene molecule and its concentration (Figure 9) (Spillmann et al., 2009).

To improve cellular targeting and potential sensor applications, a bioinspiring technique was improved to obtain "nanocorals" (Basche et al., 2015). The nanocorals were obtained by using CP polystyrene nanoarrays that were etched by plasma ions to cause shrinkage and surface fissures.

After the nanostructures are coated with an Au coating of characteristic thickness, they are removed from the support material with a sonicator. Antibodies for anti-HER2 were attached to the PS patterns, and the structures showed attachments to breast cancer cell line BT474. The

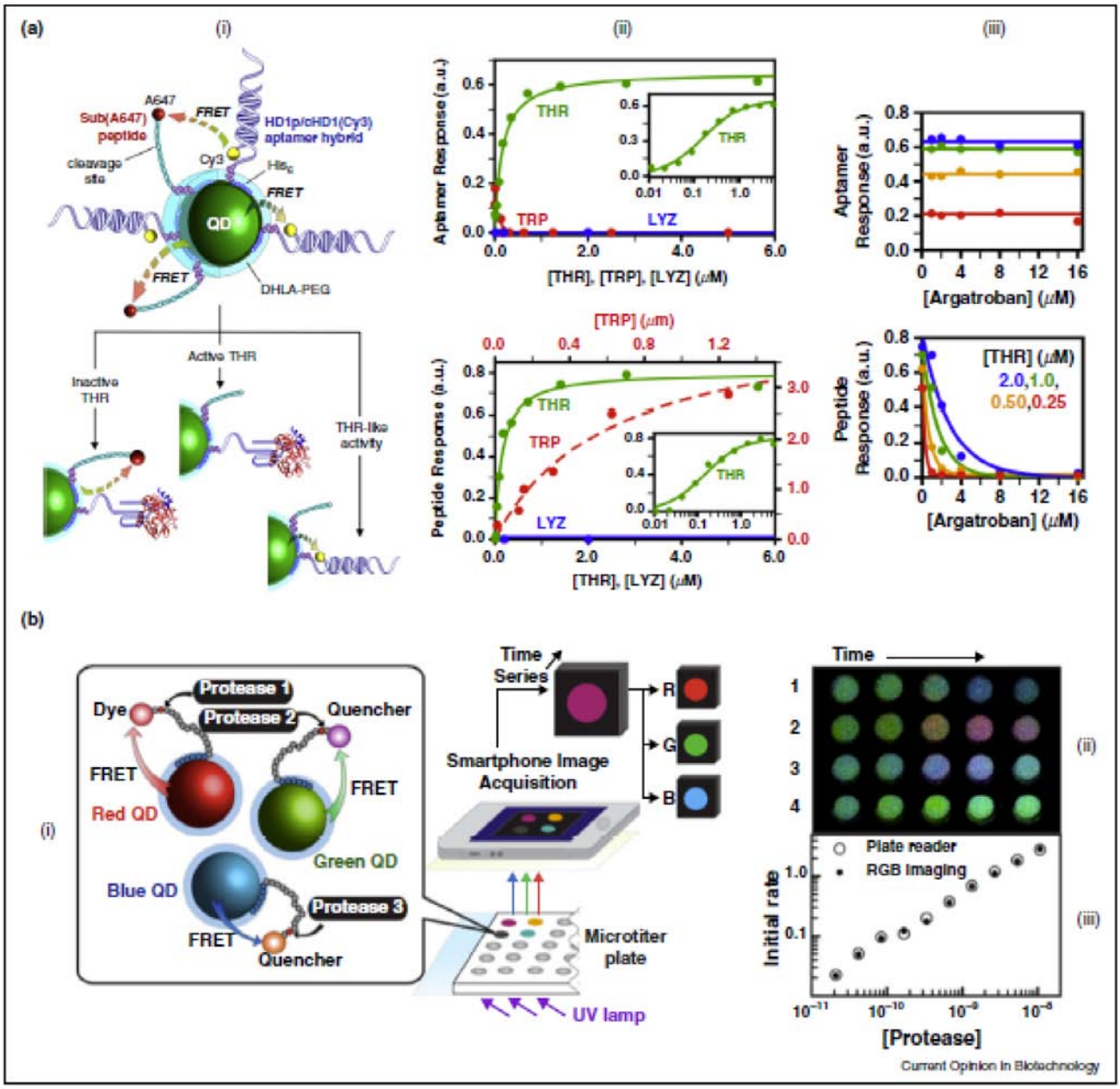

Figure 8. Current examples of QDs with novel assay formats. (a) cFRET probe is given for the parallel detection of thrombin activity and concentration: i) probe design and sensing mechanism; ii) data discriminating between thrombin, trypsin (an enzyme with thrombin-like activity), and lysozyme (a nonproteolytic enzyme); iii) data showing that whereas the peptide reaction to thrombin activity is altered, a bilateral inhibition, the aptamer reaction to thrombin concentration is unchanged by argatroban. Reprinted (adapted) with permission from Petryayeva et al. (2014). Copyright 2014 American Chemical Society. (b) FRET-based homogeneous assays for proteolytic activity utilizing the red-green-blue (RGB) color filters of a smartphone camera: i) assay format; ii) representative smartphone images for four samples at five time points; and iii) comparison of copy assays between a fluorescent plate reader and smartphone RGB imaging. Reprinted (adapted) with permission from Petryayeva et al. (2014). Copyright 2014 American Chemical Society.

antibody bonding on the PS pattern is significantly helpful due to only needing washing and incubation.

The thickness and roughness of the Au surface is a determinant factor for SERS measurement. PS as a templating material was also used to make magnetically directed nanocapsules that could pass through tumors and deliver drugs on demand (Jiang et al., 2009). IONPs of 10 nm were incorporated into PS spheres, so they were covered with a silica shell. The anticancer drug was encapsulated within the particle, since the PS structure

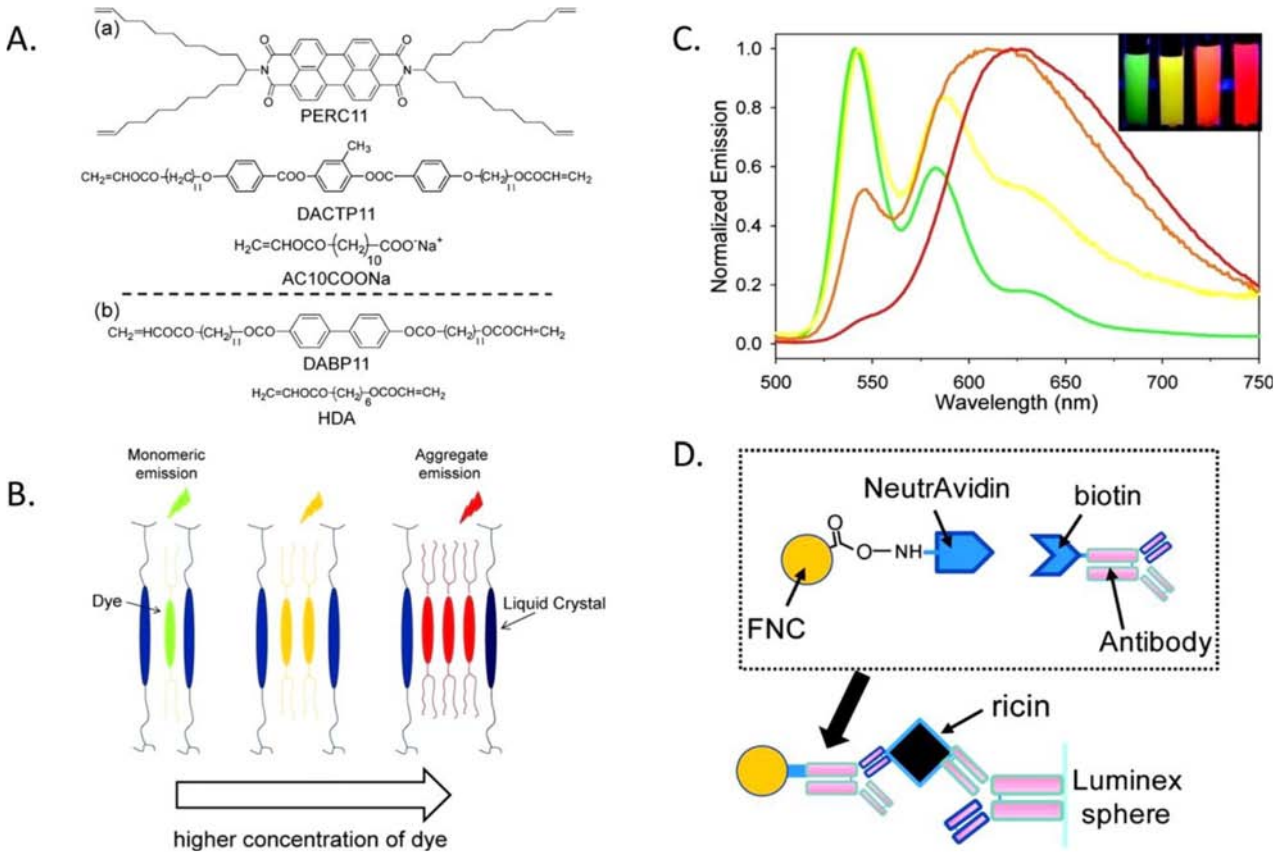

Figure 9. Liquid crystalline NPs. (A) Molecular structures of liquid crystal NPs are shown in (a) perylene tetracarboxylate diimide derivative PERC11, liquid crystalline diacrylate cross-linking agent DACTP11, and polymerizable carboxylate surfactant AC10COONa. (b) Also cross-linking agents DABP11 and HDA. (B) Dye and cross-linking agent interaction is depicted. The dye to cross-linker ratio is proportional to formation and a red shift in the emission spectrum. (C) The ratio of PERC11 to cross-linker in the nanocolloids is proportional with controllably red shifts the emission spectra. 0.6 (green), 1.5 (yellow), 2.5 (orange), and 4.8 (red) mol % of PERC11 are found place in emission spectra of populations. (D) Fluorescent nanocrystal–NeutrAvidin connected to biotinylated antiricin antibody to form a sandwich immunoassay. Reprinted (adapted) with permission from Spillmann et al. (2009). Copyright 2009 American Chemical Society.

was either dissolved or melted. The magnetic features were then developed in two techniques: actively canalizing drug capsules against a tumor cell bulk and operating the penetration of the drug from the less porous silica shell.

4. Coatings

An interesting alternative method is based on a precoated surface with a thin gold layer for functionalizing IONPs. By a variety of methods, the IO-core Au-shell NP (IONP@Au) systems have been improved (Kiatkamjornwong et al., 2002; Kim et al., 2011; Harris et al., 2015). Most techniques are achieved by the crystallization of Au grains over an IO nanocrystal and gold plating based on electrolysis. The gold coating is more permanent than polymers or monomolecular ligand shells directly bound to the IO nanoparticle's shell. Moreover, Au shell structures have intriguing optical properties (Kim et al., 2014) and show distinct magnetic properties with IONPs (Kim et al., 2011). The IONP@Au obtainment process can be modified by using classical hybridization methods, upon preparation of the Au layer, to promote the rapid formation of Au–S bonds (Bowden et al., 1999), for example by applying dithiobis(succinimidyl propionate), which can provide amine reactive succinimidyl fragments by thiolation of antibodies on the gold shell of IONP@Au after the first modification step with the heterobifunctional group (Kiatkamjornwong et al., 2002; Kim et al., 2014).

IONP@Au was initially functionalized with a mercaptopropionic group to form carboxyl acid groups on the surface, where antibodies can be hybridized through EDC/NHS chemistry with a Ni(II)-NTA structure for keeping His-tagged proteins (Adams et al., 1998; Christman et al., 2006; Ahmed et al., 2014) (Figure 10) (Deng et al., 2009). Cysteine-containing peptides have

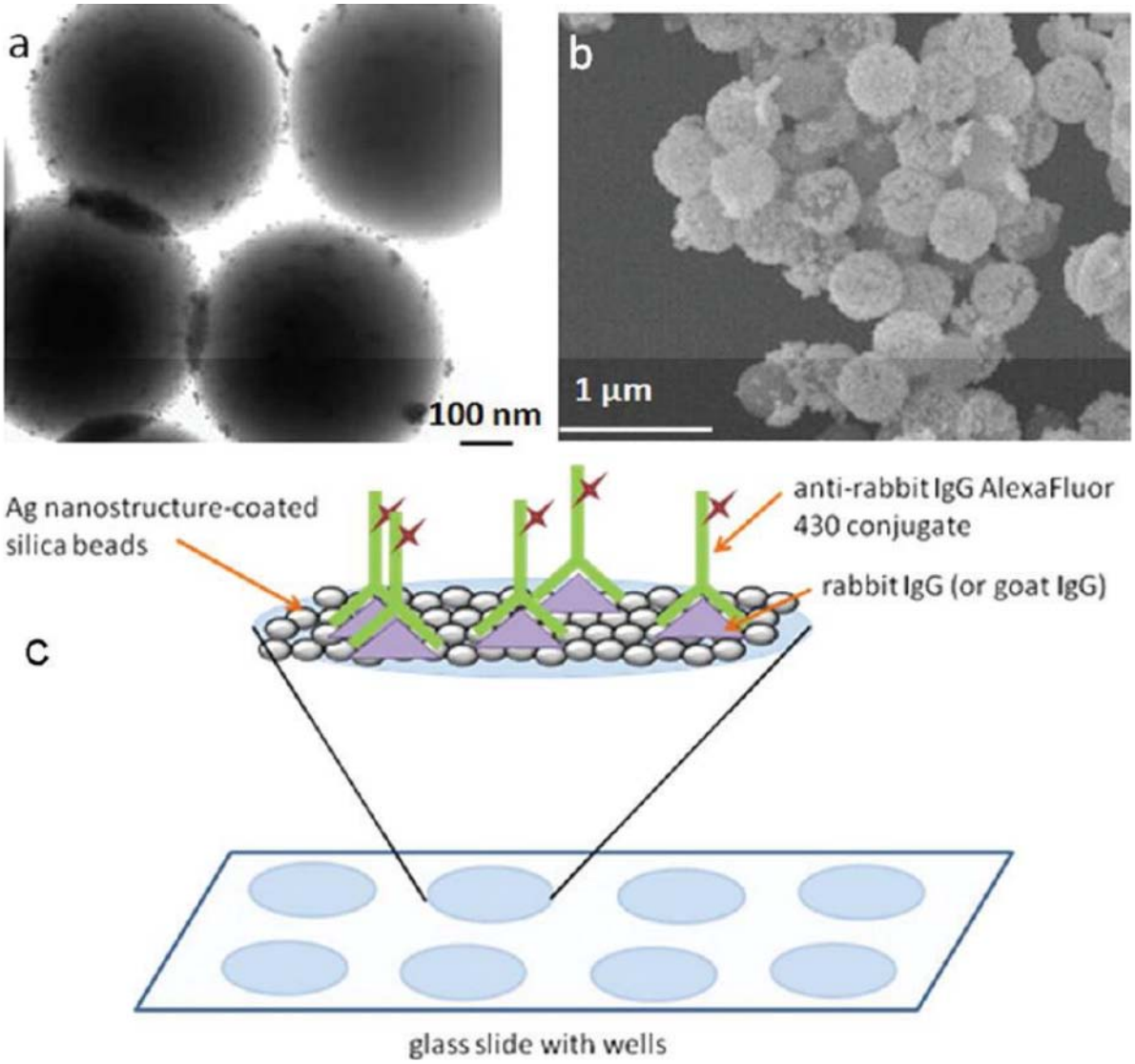

Figure 10. (a) Au-coated and (b) Ag nanostructure coated silica beads are shown in TEM images. (c) The immunoassay on a glass slide is represented. Reprinted (adapted) with permission from Deng et al. (2009). Copyright 2009 American Chemical Society.

also been directly attached to the Au shell through thiolate chemistry (De Juan-Franco et al., 2013). A surface covered by boronic acid functional groups, as another example, was prepared on the structure of IONP@Au by hybridization to a moderate mercaptopropionic group. The following step for boronic acids was practical hybridization application of diols under briefly basic conditions (Aubin-Tam and Hamad-Schifferli, 2008).

Initially, Au colloid was prepared as a seed to build a covalent bond with (3-aminopropyl)trimethoxysilane covering silica microspheres (400 nm and 5 µm in diameter; Figure 10a (Deng et al., 2009)), and also covered by a silver shell overcoating (Figure 10b (Deng et al., 2009)). An IgG rabbit antibody was used as an example of immunoassay and then labeled with Alexa Fluor 430 to examine the capability of these nanostructured systems to increase fluorescence signals on glass surfaces (Figure 10c (Deng et al., 2009)). The enhancement factor established on the fluorescence spectra on the surface of silica beads without modification was also measured as the ratio of the checked fluorescence intensity on the silver shell of silica beads. First, the fluorescence intensities were obtained from the wells structured with deposited Ag and unmodified silica beads on glass slides. These structures were also used as control samples without immunoassay. Then remarkable fluorescence results of Alexa Fluor 430-labeled IgG antibodies were obtained from one well after immunoassay hybridization and followed by washing.

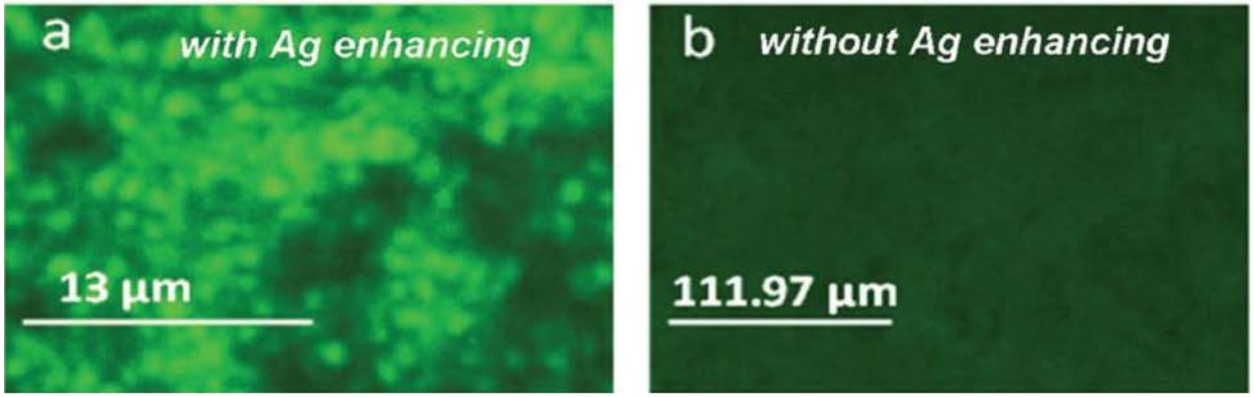

Figure 11. (a) Samples with 3 min of Ag enhancement and (b) samples without Ag enhancement, indicated by laser scanning microscopy images. Reprinted (adapted) with permission from Deng et al. (2009). Copyright 2009 American Chemical Society.

They were compared with obtained fluorescence intensities of the original Alexa Fluor 430-labeled protein suspensions under similar experimental conditions. The extent of the protein hybridization (hybridization efficiency) on the surface of silica beads with and without Ag coating was calculated. After this process, the obtained fluorescence intensity from the wells for one biosubstrate, found by matching hybridization efficiency, was interpreted to obtain the accepted fluorescence intensity. The result was equal to the fluorescence intensity required to uniformly cover the whole glass substrate for the distinct samples. Finally, the checked fluorescence intensities from the pattern immunoassay over silica particles were compared with the signal boost from silver coating the silica particles. The mean enhancement from 400 nm silica particles with 3 min of enhancement from Ag was 8.5. The enhancement factor was about 10.1 for large 5 µm silica particles, with 3 min signal acquisition after silver enhancement.

To show enhancement of fluorescence intensities from the samples with Ag coating at a 405 nm wavelength, laser scanning microscopy was utilized. The fluorescence intensities obtained from silver-coated areas were higher than those obtained from the silica particle surface only when the signal acquisition time was continued up to 3 min.

In Figure 11 (Deng et al., 2009), the fluorescence enhancement is shown. Also, the flow cytometry results of the immunoassay system are demonstrated. The enhancement was improved by controlling the fluorescence-intensity histograms of silica beads coated with Ag nanostructures and control samples.

5. Conclusions and perspective

In chemical and biological fields, the unique physical/chemical features and functionality of nanosystems are exploited and manipulated for desired aims. At the intersection of materials science, nanoscience, and biology, colloidal biohybrid systems provide a practical advancing research field. Advanced medical diagnosis and therapeutic applications, including drug delivery and detection of proteins and genes, can be achieved and improved with the use of biohybrid nanoparticles because NPs and biomolecules generally have similar size scales. For example, single nucleotide polymorphisms and trinucleotide repeats are especially significant for the detection of disease-related genes and early diagnosis. Detection techniques based on nucleic acids also have significant research potential. On the other hand, it is crucial to improve analytical techniques that are sensitive, practical, and cheap for all these needs as well. This review presents the current improvements of nucleotide- and protein-detection approaches, based on nanomaterials, used in some analytic methods including colorimetry, fluorescence-based methods, electrochemistry, microarray methods, SERS, and QCM methods. Samples involving a variety of components and biological species are more complex mixtures to be examined. Thus, monitoring or detecting the molecule of interest in bodily fluids (i.e. blood, serum, plasma, and urea) is quite challenging. Before detection, the use of these methods requires pretreatment processes, such as separation, purification, accumulation, and amplification. Significantly, the pretreatment processes might be improved and simplified at the same time by the convenient employment of nanomaterials. These current improvements provide great prospects for clinical studies on next-generation disease-detection methods based on nanobiohybrid systems.

Acknowledgment

This research was supported by grants from Harran University.

References

Ackerson BJ (1990). Shear-induced order of hard sphere suspensions. J Phys-Condens Mat 2: 389.

Adams M, Dogic Z, Keller SL, Fraden S (1998). Entropically driven microphase transitions in mixtures of colloidal rods and spheres. Nature 393: 349-352.

Ahmadivand A (2012). Routing properties of the T-structure based on Au/SiO2 nanorings in optical nanophotonic devices. Opt Appl 42: 659-666.

Ahmadivand A, Golmohammadi S, Rostami A (2012). T- and Y-splitters based on an Au/SiO2 nanoring chain at an optical communication band. Appl Optics 51: 2784-2793.

Ahmed M, Guleria A, Rath MC, Singh AK, Adhikari, S, Sarkar SK (2014). Facile and green synthesis of CdSe quantum dots in protein matrix: tuning of morphology and optical properties. J Nanosci Nanotechno 14: 5730-5742.

Aime C, Coradin T (2012). Nanocomposites from biopolymer hydrogels: blueprints for white biotechnology and green materials chemistry. J Polym Sci Pol Phys 50: 669-680.

Algar WR, Susumu K, Delehanty JB, Medintz IL (2011). Semiconductor quantum dots in bioanalysis: crossing the valley of death. Anal Chem 83: 8826-8837.

Ali K, Ahmed B, Dwivedi S, Saquib Q, Al-Khedhairy AA, Musarrat J (2015). Microwave-accelerated green synthesis of stable silver nanoparticles with *Eucalyptus globulus* leaf extract and their antibacterial and antibiofilm activity on clinical isolates. PLoS One 10: e0131178.

Amiri AM, Shanbedi G, Ahmadi H, Eshghi BT, Kazi SN (2015). Microwave-assisted direct coupling of graphene nanoplatelets with poly ethylene glycol and 4-phenylazophenol molecules for preparing stable-colloidal system. Colloid Surface A 487: 131-141.

André RM, Warren-Smith SC, Becker M, Dellith J, Rothhardt M, Zibaii MI, Latifi H, Marques MB, Bartelt H, Frazão O (2016). Simultaneous measurement of temperature and refractive index using focused ion beam milled Fabry-Perot cavities in optical fiber micro-tips. Opt Express 24: 14053-14065.

Arsenault A, Fournier-Bidoz SB, Hatton B, Miguez H, Tetrault N, Vekris E, Wong S, Yang SM, Kitaev V, Ozin GA (2004). Towards the synthetic all-optical computer: science fiction or reality? J Mater Chem 14: 781-794.

Askar K, Phillips BM, Fang Y, Choi B, Gozubenli N, Jiang P, Jiang B (2013). Self-assembled self-cleaning broadband anti-reflection coatings. Colloid Surface A 439: 84-100.

Aubin-Tam ME, Hamad-Schifferli K (2008). Structure and function of nanoparticle–protein conjugates. Biomed Mater 3: 034001.

Baffa R, Fassan M, Volinia S, O'Hara B, Liu CG, Palazzo JP, Gardiman M, Rugge M, Gomella LG, Croce CM et al. (2009). MicroRNA expression profiling of human metastatic cancers identifies cancer gene targets. J Pathol 219: 214-221.

Baldassarre F, Cacciola M, Ciccarella G (2015). A predictive model of iron oxide nanoparticles flocculation tuning Z-potential in aqueous environment for biological application. J Nanopart Res 17:1-9.

Banarjee S, Dionysiou D, Pillai S (2015). Self-cleaning applications of TiO2 by photo-induced hydrophilicity and photocatalysis. Appl Catal B-Environ 176-177: 396-428.

Bardosova M, Pemble ME, Povey IM, Tredgold RH (2010). The Langmuir-Blodgett approach to making colloidal photonic crystals from silica spheres. Adv Mater 22: 3104-3124.

Bartel DP (2009). MicroRNAs: Target recognition and regulatory functions. Cell 136: 215-233.

Basche T, Bottin A, Li C, Muellen K, Kim JH, Sohn BH, Prabhakaran P, Lee KS (2015). Energy and charge transfer in nanoscale hybrid materials. Macromol Rapid Comm 36: 1026-1046.

Baxter SM, Sperry PR, Fu ZW (1997). Partitioning of polymer and inorganic colloids in two-phase aqueous polymer systems. Langmuir 13: 3948-3952.

Bhatia P, Yadav P, Gupta BD (2013). Surface plasmon resonance based fiber optic hydrogen peroxide sensor using polymer embedded nanoparticles. Sensor Actuat B-Chem 182: 330-335.

Bhattacharya P, Lin SJ, Turner JP, Ke PC (2010). Physical adsorption of charged plastic nanoparticles affects algal photosynthesis. J Phys Chem C 114: 16556-16561.

Bhattacharya R, Mukherjee P (2008). Biological properties of "naked" metal nanoparticles. Adv Drug Deliver Rev 60: 1289-1306.

Blanco A, Chomski E, Grabtchak S, Ibisate M, John S, Leonard SW, Lopez C, Meseguer F, Miguez H, Mondia JP et al. (2000). Large-scale synthesis of a silicon photonic crystal with a complete three-dimensional bandgap near 1.5 micrometres. Nature 405: 437-440.

Bong KW, Kim JJ, Cho H, Lim E, Doyle PS, Irimia D (2015). Synthesis of cell-adhesive anisotropic multifunctional particles by stop flow lithography and streptavidin-biotin interactions. Langmuir 31: 13165-13171.

Boulares-Pender A, Prager-Duschke A, Elsner C, Buchmeiser MR (2009). Surface-functionalization of plasma-treated polystyrene by hyperbranched polymers and use in biological applications. J Appl Polym Sci 112: 2701-2709.

Bowden N, Choi IS, Grzybowski BA, Whitesides GM (1999). Mesoscale self-assembly of hexagonal plates using lateral capillary forces: Synthesis using the capillary bond. J Am Chem Soc 121: 5373-5391.

Bowers MJ, McBride JR, Rosenthal SJ (2005). White-light emission from magic-sized cadmium selenide nanocrystals. J Am Chem Soc 127: 15378-15379.

Brands M, Carl A, Dumpich G (2005). Preparation of large area sub-50 nm polymer nanoring arrays. Superlattice Microst 37: 388-393.

Breitling F, Felgenhauer T, Nesterov A, Lindenstruth V, Stadler V, Bischoff FR (2009). Particle-based synthesis of peptide arrays. ChemBioChem 10: 803-808.

Budkowski A, Bernasik A, Moons E, Lekka M, Zemla J, Jaczewska J, Haberko J, Raczkowska J, Rysz J (2009). Structures in multicomponent polymer films: Their formation, observation and applications in electronics and biotechnology. Acta Phys Pol A 115: 435-440.

Budkowski A, Zemla J, Moons E, Awsiuk K, Rysz J, Bernasik A, Bjorstrom-Svanstrom CM, Lekka M, Jaczewska J (2012). Polymer blends spin-cast into films with complementary elements for electronics and biotechnology. J Appl Polym Sci 125: 4275-4284.

Cennamo N, Massarotti D, Galatus R, Conte L, Zeni L (2013). Performance comparison of two sensors based on surface plasmon resonance in a plastic optical fiber. Sensors 13: 721-735.

Chen JY, Chao DM, Lu XF, Zhang WJ, Manohar SK (2006). General synthesis of two-dimensional patterned conducting polymer-nanobowl sheet via chemical polymerization. Macromol Rapid Comm 27: 771-775.

Chen Q, Bae SC, Granick S (2011). Directed self-assembly of a colloidal kagome lattice. Nature 469: 381-384.

Chen SY, Yen YT, Chen YY, Hsu CS, Chueh YL, Chen LJ (2012). Large scale two-dimensional nanobowl array high efficiency polymer solar cell. RSC Advances 2: 1314-1317.

Chen TH, Tsai TY, Hsieh KC, Chang SC, Tai NH, Chen HL (2008). Two-dimensional metallic nanobowl array transferred onto thermoplastic substrates by microwave heating of carbon nanotubes. Nanotechnology 19: 465303.

Chen X, Wei X, Jiang K (2008). Large-scale fabrication of ordered metallic hybrid nanostructures. Opt Express 16: 11888-11893.

Chen YC, Zhou SX, Yang HH, Wu LM (2005). Structure and properties of polyurethane/nanosilica composites. J Appl Poly Sci 95: 1032-1039.

Cheng J, Tang X, Zhao J, Shi T, Zhao P, Lin C (2016). Multifunctional cationic polyurethanes designed for non-viral cancer gene therapy. Acta Biomater 30: 155-167.

Cheng X, Lowe SB, Reece PJ, Gooding JJ (2014). Colloidal silicon quantum dots: from preparation to the modification of self-assembled monolayers (SAMs) for bio-applications. Chem Soc Rev 43: 2680-2700.

Cheng X, McCoy JH, Israelachvili JN, Cohen I (2011). Imaging the microscopic structure of shear thinning and thickening colloidal suspensions. Science 333: 1276-1279.

Christman KL, Requa MV, Enriquez-Rios VD, Ward SC, Bradley KA, Turner KL, Maynard HD (2006). Submicron streptavidin patterns for protein assembly. Langmuir 22: 7444-7450.

Chung K, Lee J, Lee JE, Lee JY, Moon S, Lau KHA, Kim D, Kim DH (2013). A simple and efficient strategy for the sensitivity enhancement of DNA hybridization based on the coupling between propagating and localized surface plasmons. Sensor Actuat B-Chem 176: 1074-1080.

Coppage R, Slocik JM, Briggs BD, Frenkel AI, Naik RR, Knecht MR (2012). Determining peptide sequence effects that control the size, structure, and function of nanoparticles. ACS Nano 6: 1625-1636.

Cutler PJ, Malik MD, Liu S, Byars JM, Lidke DS, Lidke KA (2013). Multi-color quantum dot tracking using a high-speed hyperspectral line-scanning microscope. PLoS ONE 8: e64320.

Dalton L, Harper A, Ren A, Wang F, Todorova G, Chen J, Zhang C, Lee M (1999). Polymeric electro-optic modulators: From chromophore design to integration with semiconductor very large scale integration electronics and silica fiber optics. I&EC Research 38: 8-33.

De Azevedo WM, de Oliveira Luna AJH, Silva EFVBN, Silva RO (2006). The effect of ultrasonic waves in conducting polymer solution. Ultrason Sonochem 13: 433-437.

De Backer L, Braeckmans K, Stuart MCA, Demeester J, De Smedt SC, Raemdonck K (2015). Bio-inspired pulmonary surfactant-modified nanogels: A promising siRNA delivery system. J Control Release 206: 177-186.

De Juan-Franco E, Caruz A, Pedrajas JR, Lechuga LM (2013). Site-directed antibody immobilization using a protein A-gold binding domain fusion protein for enhanced SPR immunosensing. Analyst 138: 2023-2031.

Del Mercato LL, Guerra F, Lazzari G, Nobile C, Bucci C, Rinaldi R (2016). Biocompatible multilayer capsules engineered with a graphene oxide derivative: synthesis, characterization and cellular uptake. Nanoscale 8: 7501-7512.

Deng W, Drozdowicz-Tomsia K, Jin D, Goldys EM (2009). Enhanced flow cytometry-based bead immunoassays using metal nanostructures. Anal Chem 81: 7248-7255.

Devetter BM, Mukherjee P, Murphy CJ, Bhargava R (2015). Measuring binding kinetics of aromatic thiolated molecules with nanoparticles via surface-enhanced Raman spectroscopy. Nanoscale 7: 8766-8775.

Ding W, Liu Y, Li Y, Shi Q, Li H, Xia H, Wang D, Tao X (2014). Water-soluble gold nanoclusters with pH-dependent fluorescence and high colloidal stability over a wide pH range via co-reduction of glutathione and citrate. RSC Advances 4: 22651-22659.

Dou X, Phillips BM, Chung PY, Jiang P (2012). High surface plasmon resonance sensitivity enabled by optical disks. Opt Letters 37: 3681-3683.

Dziubakiewicz E, Hrynkiewicz K, Walczyk M, Buszewski B (2013). Study of charge distribution on the surface of biocolloids. Colloid Surface B 104: 122-127.

Elsabahy M, Wooley KL (2013). Cytokines as biomarkers of nanoparticle immunotoxicity. Chem Soc Rev 42: 5552-5576.

Farkhani SM, Valizadeh A (2014). Review: three synthesis methods of CdX (X = Se, S or Te) quantum dots. IET Nanobiotechnol 8: 59-76.

Fen YW, Yunus WMM (2013). Utilization of chitosan-based sensor thin films for the detection of lead ion by surface plasmon resonance optical sensor. IEEE Sens J 13: 1413-1418.

Ferreira RV, Silva-Caldeira PP, Pereira-Maia EC, Fabris JD, Cavalcante LCD, Ardisson JD, Domingues RZ (2016). Bio-inactivation of human malignant cells through highly responsive diluted colloidal suspension of functionalized magnetic iron oxide nanoparticles. J Nanopart Res 18: 4-10.

Filip D, Macocinschi D, Paslaru E, Tuchilus CG, Vlad S (2016). Surface characterization and antimicrobial properties of sodium deoxycholate-based poly(ester ether)urethane ionomer biomaterials. React Funct Polym 102: 70-81.

Frank B, Yin X, Schäferling M, Zhao J, Hein SM, Braun PV, Giessen H (2013). Large-area 3D chiral plasmonic structures. ACS Nano 7: 6321-6329.

Fudouzi H, Sawada T (2006). Photonic rubber sheets with tunable color by elastic deformation. Langmuir 22: 1365-1368.

Gabudean AM, Biro D, Astilean S (2012). Hybrid plasmonic platforms based on silica-encapsulated gold nanorods as effective spectroscopic enhancers for Raman and fluorescence spectroscopy. Nanotechnology 23: 485706.

Gadegaard N, Martines E, Riehle MO, Seunarine K, Wilkinson CDW (2006). Applications of nano-patterning to tissue engineering. Microelectron Eng 83: 1577-1581.

Garg R, Tripathi SM, Thyagarajan K, Bock WJ (2013). Long period fiber grating based temperature-compensated high performance sensor for bio-chemical sensing applications. Sensor Actuat B 176: 1121-1127.

Garg T (2016). Current nanotechnological approaches for an effective delivery of bio-active drug molecules in the treatment of acne. Artif Cell Nanomed Sub 44: 98-105.

Garrido C, Weiss-Lopez BE, Campos Vallette MM (2016). Surface-enhanced Raman scattering activity of negatively charged bio-analytes from a modified silver colloid. Spectrosc Lett 49: 11-18.

Gatto E, Formaggio F, Toniolo C, Venanzi M (2013). Self-assembled monolayers formed by conformationally constrained oligopeptides A new tool for bioinspired nanotechnology. Chim Oggi 31: 27-31.

Ghosh A, Collie SR (2014). Keratinous materials as novel absorbent systems for toxic pollutants. Defence Sci J 64: 209-221.

Giorgetti E, Muniz-Miranda M, Marsili P, Scarpellini D, Giammanco F (2012). Stable gold nanoparticles obtained in pure acetone by laser ablation with different wavelengths. J Nanopart Res 14: 648.

Gioux S, Choi HS, Frangioni JV (2010). Image-guided surgery using invisible near-infrared light: fundamentals of clinical translation. Mol Imaging 9: 237.

Gonella G, Dai HL (2014). Second harmonic light scattering from the surface of colloidal objects: theory and applications. Langmuir 30: 2588-2599.

Griesser HJ, Hartley PG, McArthur SL, McLean KM, Meagher L, Thissen H (2002). Interfacial properties and protein resistance of nano-scale polysaccharide coatings. Smart Mater Struct 11: 652-661.

Gui R, Jin H, Wang Z, Tan L (2015). Recent advances in synthetic methods and applications of colloidal silver chalcogenide quantum dots. Coordin Chem Rev 296: 91-124.

Guisbiers G, Wang Q, Khachatryan E, Arellano-Jimenez MJ, Webster TJ, Larese-Casanova P, Nash KL (2015). Anti-bacterial selenium nanoparticles produced by UV/VIS/NIR pulsed nanosecond laser ablation in liquids. Laser Phys Lett 12: 016003.

Han JW, Gurunathan S, Jeong JK, Choi YJ, Kwon DN, Park JK, Kim JH (2014). Oxidative stress mediated cytotoxicity of biologically synthesized silver nanoparticles in human lung epithelial adenocarcinoma cell line. Nanoscale Res Lett 9: 459.

Han Y, Fan C, Wu G, Chen H, Wang M (2011). Low-temperature solution processed ultraviolet photodetector based on ordered tio2 nanorods array-polymer hybrid. J Phys Chem C 115: 13438-13445.

Harris D (2004). Assessment of Paint Layers by Fe-Sem and Eds Examination. 18th ed. Adelphi, MD, USA: US Army Research Laboratory.

Harris RA, van der Walt H, Shumbula PM (2015). Engineered inorganic/organic-core/shell magnetic FexOy nanoparticles with oleic acid and/or oleylamine as capping agents. Curr Pharm Design 21: 5369-5388.

Hasany SF, Abdurahman NH, Sunarti AR, Jose R (2013). Magnetic iron oxide nanoparticles: chemical synthesis and applications review. Curr Nanosci 9: 561-575.

Hashemizadeh S, Huyeh MR (2014). Silver nanocolloid: synthesis, optical and thermo-optical properties. Ultrafine Nano-Str Mater 829: 670-674.

Hassan S, Singh AV (2014). Biophysicochemical Perspective of nanoparticle compatibility: a critically ignored parameter in nanomedicine. J Nanoscience Nanotechno 14: 402-414.

Haynes CL, Van Duyne RP (2001). Nanosphere lithography: a versatile nanofabrication tool for studies of size-dependent nanoparticle optics. J Phys Chem B 105: 5599-5611.

Hayward RC, Saville DA, Aksay IA (2000). Electrophoretic assembly of colloidal crystals with optically tunable micropatterns. Nature 404: 56-59.

He S, Lu C, Zhang S (2011). Facile and efficient route to polyimide-tio2 nanocomposite coating onto carbon fiber. Acs Appl Mater Inter 3: 4744-4750.

Helmbrecht C, Luetzenkirchen-Hecht D, Frank W (2015). Microwave-assisted synthesis of water-soluble, fluorescent gold nanoclusters capped with small organic molecules and a revealing fluorescence and X-ray absorption study. Nanoscale 7: 4978-4983.

Heo CJ, Kim SH, Jang SG, Lee SY, Yang SM (2009). Gold "nanograils" with tunable dipolar multiple plasmon resonances. Adv Mater 21: 1726-1731.

Hermanson GT (2013). Bioconjugate Techniques. 1st ed. London, UK: Academic Press.

Herold C, Leduc C, Stock R, Diez S, Schwille P (2012). Long-range transport of giant vesicles along microtubule networks. ChemPhysChem 13: 1001-1006.

Ho K, Chan CT, Soukoulis CM (1990). Existence of a photonic gap in periodic dielectric structures. Phys Rev Lett 65: 3152.

Holland BT, Blanford CF, Stein A (1998). Synthesis of macroporous minerals with highly ordered three-dimensional arrays of spheroidal voids. Science 281: 538-540.

Holtz JH, Asher SA (1997). Polymerized colloidal crystal hydrogel films as intelligent chemical sensing materials. Nature 389: 829-832.

Homola J (2006). Surface plasmon resonance (SPR) biosensors and their applications in food safety and security. NATO Sci Ser II Math 216: 101-118.

Homola J (2008). Surface plasmon resonance sensors for detection of chemical and biological species. Chem Rev 108: 462-493.

Howes PD, Chandrawati R, Stevens MM (2014). Colloidal nanoparticles as advanced biological sensors. Science 346: 53.

Hussain S, Akrema, Rahisuddin, Khan Z (2014). Extracellular biosynthesis of silver nanoparticles: effects of shape-directing cetyltrimethylammonium bromide, pH, sunlight and additives. Bioproc Biosyst Eng 37: 953-964.

Hvastkovs EG, Schenkman JB, Rusling JF (2012). Metabolic toxicity screening using electrochemiluminescence arrays coupled with enzyme-DNA biocolloid reactors and liquid chromatography-mass spectrometry. Annu Rev Anal Chem 5: 79-105.

Im H, Lee SH, Wittenberg NJ, Johnson TW, Lindquist NC, Nagpal P, Norris DJ, Oh SH (2011). Template-stripped smooth Ag nanohole arrays with silica shells for surface plasmon resonance biosensing. ACS Nano 5: 6244-6253.

Jang KS, Kim JD (2011). An anionic surfactant-templated synthesis and lamellar ordering of Co(OH)2 and Co3O4 nanodisks. Mater Chem Phys 125: 777-783.

Jang SG, Choi DG, Heo CJ, Lee SY, Yang SM (2008). Nanoscopic ordered voids and metal caps by controlled trapping of colloidal particles at polymeric film surfaces. Adv Mater 20: 4862-4867.

Janib SM, Moses AS, MacKay JA (2010). Imaging and drug delivery using theranostic nanoparticles. Adv Drug Deliver Rev 62: 1052-1063.

Jethmalani JM, Ford WT, Beaucage G (1997). Crystal structures of monodisperse colloidal silica in poly(methyl acrylate) films. Langmuir 13: 3338-3344.

Jia G, Xu S, Wang A (2015). Emerging strategies for the synthesis of monodisperse colloidal semiconductor quantum rods. J Mater Chem C 3: 8284-8293.

Jiang K, Wang Y, Dong J, Gui L, Tang Y (2001). Electrodeposited metal sulfide semiconductor films with ordered nanohole array structures. Langmuir 17: 3635-3638.

Jiang P, Bertone J, Hwang K, Colvin V (1999). Single-crystal colloidal multilayers of controlled thickness. Chem Mater 11: 2132-2140.

Joannopoulos JD, Johnson SG, Winn JN, Meade RD (2011). Photonic Crystals: Molding the Flow of Light. 2nd ed. Princeton, NJ, USA: Princeton University Press.

Johnson CM, Pate KM, Shen Y, Viswanath A, Tan R, Benicewicz BC, Moss MA, Greytak AB (2015). A methacrylate-based polymeric imidazole ligand yields quantum dots with low cytotoxicity and low nonspecific binding. J Colloid Interf Sci 458: 310-314.

Johnson L, Walsh DA (2011). Deposition of silver nanobowl arrays using polystyrene nanospheres both as reagents and as the templating material. J Mater Chem 21: 7555-7558.

Jokinen M, Pätsi M, Rahiala H, Peltola T, Ritala M, Rosenholm J (1998). Influence of sol and surface properties on in vitro bioactivity of sol-gel-derived TiO_2 and TiO_2-SiO_2 films deposited by dip-coating method. J Biomed Mater Res 42: 295-302.

Juang RS, Lin KH (2004). Ultrasound-assisted production of W/O emulsions in liquid surfactant membrane processes. Colloid Surface A 238: 43-49.

Kainz B, Steiner K, Sleytr UB, Pum D, Toca-Herrera JL (2010). Fluorescence energy transfer in the bi-fluorescent S-layer tandem fusion protein ECFP–SgsE–YFP. J Struct Bio 172: 276-283.

Kajihara K, Yao T (2000). Macroporous morphology of the titania films prepared by a sol-gel dip-coating method from the system containing poly (ethylene glycol). J Sol-Gel Sci Techn 17: 173-184.

Kalsin AM, Fialkowski M, Paszewski M, Smoukov SK, Bishop KJM, Grzybowski BA (2006). Electrostatic self-assembly of binary nanoparticle crystals with a diamond-like lattice. Science 312: 420-424.

Kang D, Cai Z, Jin Q, Zhang H (2015). Bio-inspired composite films with integrative properties based on the self-assembly of gellan gum-graphene oxide crosslinked nanohybrid building blocks. Carbon 91: 445-457.

Kaombe DD, Hagg MB (2014). Forward osmosis for the dewatering of pyrolysis oil aqueous phase. Sep Purif Technol 138: 92-97.

Karatutlu A, Little W, Ersoy O, Zhang Y, Seker I, Sapelkin A (2015). Laser-induced particle size tuning and structural transformations in germanium nanoparticles prepared by stain etching and colloidal synthesis route. J Appl Phys 118: 244303.

Khiyami MA, Almoammar H, Awad YM, Alghuthaymi MA, Abd-Elsalam KA (2014). Plant pathogen nanodiagnostic techniques: forthcoming changes? Biotechnol Biotech Eq 28: 775-785.

Kim JH (2012). A hyperlink and semantic network analysis of the triple helix (university-government-industry): the interorganizational communication structure of nanotechnology. J Comput-Mediat Comm 17: 152-170.

Kim JH, Kang SH, Zhu K, Kim JY, Neale NR, Frank AJ (2011). Ni-NiO core-shell inverse opal electrodes for supercapacitors. Chem Comm 47: 5214-5216.

Kim JS, Jeon HJ, Yoo HW, Baek YK, Kim KH, Kim DW, Jung HT (2014). Generation of monodisperse, shape-controlled single and hybrid core-shell nanoparticles via a simple one-step process. Adv Funct Mater 24: 841-847.

Kim SH, Kim SH, Jeong WC, Yang S-M (2009). Low-threshold lasing in 3D dye-doped photonic crystals derived from colloidal self-assemblies. Chem Mater 21: 4993-4999.

Klang V, Matsko NB, Valenta C, Hofer F (2012). Electron microscopy of nanoemulsions: an essential tool for characterisation and stability assessment. Micron 43: 85-103.

Knez K, Noppe W, Geukens N, Janssen KPF, Spasic D, Heyligen J, Vriens K, Thevissen K, Cammue BPA, Petrenko V et al (2013). Affinity comparison of p3 and p8 peptide displaying bacteriophages using surface plasmon resonance. Anal Chem 85: 10075-10082.

Knoblauch C, Griep M, Friedrich C (2014). Recent advances in the field of bionanotechnology: An insight into optoelectric bacteriorhodopsin, quantum dots, and noble metal nanoclusters. Sensors 14: 19731-19766.

Kostiainen MA, Hiekkataipale P, Laiho A, Lemieux V, Seitsonen J, Ruokolainen J, Ceci P (2013). Electrostatic assembly of binary nanoparticle superlattices using protein cages. Nat Nano 8: 52-56.

Koynov K, Butt H Jr (2012). Fluorescence correlation spectroscopy in colloid and interface science. Curr Opin Colloid In 17: 377-387.

Kralchevsky P, Denkov N, Paunov V, Velev O, Ivanov I, Yoshimura H, Nagayama K (1994). Formation of two-dimensional colloid crystals in liquid films under the action of capillary forces. J Phys Condens Mat 6: A395.

Krpetic Z, Anguissola S, Garry D, Kelly PM, Dawson KA (2014). Nanomaterials: impact on cells and cell organelles. Adv Exp Med Biol 2014;811: 135-156.

Kumar D, Rajeshwari A, Jadon PS, Chaudhuri G, Mukherjee A, Chandrasekaran N, Mukherjee A (2015). Cytogenetic studies of chromium (III) oxide nanoparticles on *Allium cepa* root tip cells. J Environ Sci 38: 150-157.

Kumar DA, Palanichamy V, Roopan SM (2014). Green synthesis of silver nanoparticles using Alternanthera dentata leaf extract at room temperature and their antimicrobial activity. Spectrochim Acta Part A 127: 168-171.

Lee JH, Leung W, Ahn J, Lee T, Park IS, Constant K, Ho KM (2007). Layer-by-layer photonic crystal fabricated by low-temperature atomic layer deposition. Appl Phys Lett 90: 151101.

Lee KS, Kim BY, Yoon HJ, Choi YS, Jin BR (2016). Secapin, a bee venom peptide, exhibits anti-fibrinolytic, anti-elastolytic, and anti-microbial activities. Dev Comp Immunol 63: 27-35.

Lee W, Chan A, Bevan MA, Lewis JA, Braun PV (2004). Nanoparticle-mediated epitaxial assembly of colloidal crystals on patterned substrates. Langmuir 20: 5262-5270.

Lei M, Wang SL, Li LH, Tang WH (2011). A Nafion-silica cathode electrolyte for durable elevated-temperature direct methanol fuel cells. J Power Sources 196: 1123-1126.

Li F, Lu Y, Liu L, Zhang L, Dai J, Ma J (2013). Relations between carbon nanotubes' length and their composites' mechanical and functional performance. Polymer 54: 2158-2165.

Li L, Liu J, Yang X, Huang J, He D, Guo X, Wan L, He X, Wang K (2016). Biomimetic synthesis of highly biocompatible gold nanoparticles with amino acid-dithiocarbamate as a precursor for SERS imaging. Nanotechnology 27: 105603.

Li Y, Zhang J, Fang L, Wang T, Zhu S, Li Y, Wang Z, Zhang L, Cui L, Yang B (2011). Fabrication of silicon/polymer composite nanopost arrays and their sensing applications. Small 7: 2769-2774.

Lima-Tenorio MK, Gomez Pineda EA, Ahmad NM, Fessi H, Elaissari A (2015). Magnetic nanoparticles: In vivo cancer diagnosis and therapy. Int J Pharm 493: 313-327.

Linn NC, Sun C-H, Arya A, Jiang P, Jiang B (2009). Surface-enhanced Raman scattering on periodic metal nanotips with tunable sharpness. Nanotechnology 20: 225303.

Liu K, Yao X, Jiang L (2010). Recent developments in bio-inspired special wettability. Chem Soc Rev 39: 3240-3255.

Liu X, Choi B, Gozubenli N, Jiang P (2013). Periodic arrays of metal nanorings and nanocrescents fabricated by a scalable colloidal templating approach. J Colloid Interf Sci 409: 52-58.

Liu X, Li L, Li W, Yang Y, Mao L, Liu X, Li L, Li WJ, Yang Y, Mao LG (2013). Research progress on the detection of pesticide residues by surface plasmon resonance sensor. J Food Safety Quality 4: 321-327.

Liu X, Linn NC, Sun CH, Jiang P (2010). Templated fabrication of metal half-shells for surface-enhanced Raman scattering. Phys Chem Chem Phys 12: 1379-1387.

Liu X, Sun CH, Jiang P (2010). Templated fabrication of periodic arrays of metallic attoliter petri dishes. Chem Mater 22: 1768-1775.

Liu X, Sun CH, Linn NC, Jiang B, Jiang P (2009). Wafer-scale surface-enhanced Raman scattering substrates with highly reproducible enhancement. J Phys Chem C 113: 14804-14811.

Liu XY, Mazumdar D, Schrag BD, Shen W, Xiao G (2004). Magnetization reversal of submicrometer Co rings with uniaxial anisotropy via scanning magnetoresistance microscopy. Phys Rev B 70: 014407.

Logeswari P, Silambarasan S, Abraham J (2015). Synthesis of silver nanoparticles using plants extract and analysis of their antimicrobial property. J Sau Chem Soc 19: 311-317.

Lukianova-Hleb EY, Ren X, Constantinou PE, Danysh BP, Shenefelt DL, Carson DD, Farach-Carson MC, Kulchitsky VA, Wu X, Wagner DS et al (2012). Improved cellular specificity of plasmonic nanobubbles versus nanoparticles in heterogeneous cell systems. PLoS One 7: e34537.

Luo Z, Deng Y, Zhang R, Wang M, Bai Y, Zhao Q, Lyu Y, Wei J, Wei S (2015). Peptide-laden mesoporous silica nanoparticles with promoted bioactivity and osteo-differentiation ability for bone tissue engineering. Colloid Surface B 131: 73-82.

Lynch I, Cedervall T, Lundqvist M, Cabaleiro-Lago C, Linse S, Dawson KA (2007). The nanoparticle–protein complex as a biological entity; a complex fluids and surface science challenge for the 21st century. Adv Colloid Interf Sci 134: 167-174.

Lyshevski SE (2005). Nano- and Micro-Electromechanical Systems: Fundamentals of Nano- and Microengineering. Boca Raton, FL, USA: CRC Press.

Madden O, Naughton MD, Moane S, Murray PG (2015). Mycofabrication of common plasmonic colloids, theoretical considerations, mechanism and potential applications. Adv Colloid Interf Sci 225: 37-52.

Maduraiveeran G, Ramaraj R (2013). Silver nanoparticles embedded in functionalized silicate sol-gel network film as optical sensor for the detection of biomolecules. J Anal Chem 68: 241-248.

Mahyad B, Janfaza S, Hosseini ES (2015). Bio-nano hybrid materials based on bacteriorhodopsin: potential applications and future strategies. Adv Colloid Interf Sci 225: 194-202.

Malaczewska J (2014). The in vitro effect of commercially available noble metal nanocolloids on the splenocyte proliferative response and cytokine production in mice. Pol J Vet Sci 17: 37-45.

Manera MG, Colombelli A, Rella R, Caricato A, Cozzoli PD, Martino M, Vasanelli L (2012). TiO_2 brookite nanostructured thin layer on magneto-optical surface plasmon resonance transductor for gas sensing applications. J Appl Phys 112: 053524.

Manera MG, Ferreiro-Vila E, Garcia-Martin JM, Cebollada A, Garcia-Martin A, Giancane G, Valli L, Rella R (2013). Enhanced magneto-optical SPR platform for amine sensing based on Zn porphyrin dimers. Sensor Actuat B-Chem 182: 232-238.

Mansur HS, Mansur AAP, Soriano-Araujo A, Lobato ZIP, de Carvalho SM, de Fatima Leite M (2015). Water-soluble nanoconjugates of quantum dot-chitosan-antibody for in vitro detection of cancer cells based on enzyme-free fluoroimmunoassay. Mat Sci Eng C-Mat 52: 61-71.

Martinolich AJ, Park G, Nakamoto MY, Gate RE, Wheeler KE (2012). Structural and functional effects of cu metalloprotein-driven silver nanoparticle dissolution. Environ Sci Technol 46: 6355-6362.

Massey M, Wu M, Conroy EM, Algar WR (2015). Mind your P's and Q's: the coming of age of semiconducting polymer dots and semiconductor quantum dots in biological applications. Curr Opin Biotech 34: 30-40.

Matea CT, Mocan T, Zaharie F, Iancu C, Mocan L (2015). A novel immunoglobulin G monolayer silver bio-nanocomposite. Chem Cent J 9: 11.

Mayoral R, Requena J, Moya JS, López C, Cintas A, Miguez H, Meseguer F, Vázquez L, Holgado M, Blanco Á (1997). 3D Long-range ordering in an SiO_2 submicrometer-sphere sintered superstructure. Adv Mater 9: 257-260.

McBride J, Treadway J, Feldman LC, Pennycook SJ, Rosenthal SJ (2006). Structural basis for near unity quantum yield core/shell nanostructures. Nano Lett 6: 1496-1501.

Milionis A, Ruffilli R, Bayer IS (2014). Superhydrophobic nanocomposites from biodegradable thermoplastic starch composites (Mater-Bi (R)), hydrophobic nano-silica and lycopodium spores. RSC Advances 4: 34395-34404.

Mishra P, Ray S, Sinha S, Das B, Khan MI, Behera SK, Yun SI, Tripathy SK, Mishra A (2016). Facile bio-synthesis of gold nanoparticles by using extract of *Hibiscus sabdariffa* and evaluation of its cytotoxicity against U87 glioblastoma cells under hyperglycemic condition. Biochem Eng J 105: 264-272.

Mkenzie BE, Holder SJ, Sommerdijk NAJM (2012). Assessing internal structure of polymer assemblies from 2D to 3D CryoTEM: bicontinuous micelles. Curr Opin Colloid Interf Sci 17: 343-349.

Monguzzi A, Lesci IG, Capitani GC, Santo N, Roveri N, Campione M (2014). Mineral-organic hybrid nanotubes as highly sensitive solid state optical chemical sensors. Phys Chem Chem Phys 16: 2491-2498.

Montano MD, Badiei HR, Bazargan S, Ranville JF (2014). Improvements in the detection and characterization of engineered nanoparticles using spICP-MS with microsecond dwell times. Environ Sci-Nano 1: 338-346.

Mukherjee S, Chowdhury D, Kotcherlakota R, Patra S, Vinothkumar B, Bhadra MP, Sreedhar B, Patra CR (2014). Potential theranostics application of bio-synthesized silver nanoparticles (4-in-1 system). Theranostics 4: 316-335.

Mullen DG, Banaszak Holl MM (2011). Heterogeneous ligand–nanoparticle distributions: a major obstacle to scientific understanding and commercial translation. Accounts Chem Res 44: 1135-1145.

Muller FLL, Batchelli S (2013). Copper binding by terrestrial versus marine organic ligands in the coastal plume of River Thurso, North Scotland. Eastern Coast Shelf Sci 133: 137-146.

Nel AE, Mädler L, Velegol D, Xia T, Hoek EM, Somasundaran P, Klaessig F, Castranova V, Thompson M (2009). Understanding biophysicochemical interactions at the nano–bio interface. Nature Mater 8: 543-557.

Newcomb CJ, Moyer TJ, Lee SS, Stupp SI (2012). Advances in cryogenic transmission electron microscopy for the characterization of dynamic self-assembling nanostructures. Curr Opin Colloid Interf Sci 17: 350-359.

Nishiguchi A, Matsusaki M, Akashi M (2015). Cell-cell crosslinking by bio-molecular recognition of heparin-based layer-by-layer nanofilms. Macromol Biosci 15: 312-317.

Nitta J, Steiner M (2005a). Magnetization properties of microstructured NiFe rings investigated using semiconductor/ferromagnet hybrid structures. J Supercond 18: 331-334.

Nitta J, Steiner M (2005b). Semiconductor/ferromagnet hybrid devices to probe magnetisation states in microstructured NiFe rings. Iee P-Circ Dev Sys 152: 297-300.

Nomura T (2012). Control of microbial adhesion using fine particle technology. Adv Powder Technol 23: 532-537.

Nygaard J, Munch HK, Thulstrup PW, Christensen NJ, Hoeg-Jensen T, Jensen KJ, Arleth L (2012). Metal ion controlled self-assembly of a chemically reengineered protein drug studied by small-angle X-ray scattering. Langmuir 28: 12159-12170.

Orel V, Shevchenko A, Romanov A, Tselepi M, Mitrelias T, Barnes CHW, Burlaka A, Lukin S, Shchepotin I (2015). Magnetic properties and antitumor effect of nanocomplexes of iron oxide and doxorubicin. Nanomed-Nanotechnol 11: 47-55.

Pan S, Li D, Zhao L, Schenkman JB, Rusling JF (2013). Genotoxicity-related chemistry of human metabolites of benzo[*ghi*]perylene (B[*ghi*]P) investigated using electro-optical arrays and DNA/microsome biocolloid reactors with LC-MS/MS. Chem Res Toxicol 26: 1229-1239.

Park HJ, Kang MG, Guo JL (2009). Large area high density sub-20 nm SiO2 nanostructures fabricated by block copolymer template for nanoimprint lithography. ACS Nano 3: 2601-2608.

Park S, Hamad-Schifferli K (2010). Nanoscale interfaces to biology. Curr Opin Chem Bio 14: 616-622.

Pereira SO, Barros-Timmons A, Trindade T (2014). Biofunctionalisation of colloidal gold nanoparticles via polyelectrolytes assemblies. Colloid Poly Sci 292: 33-50.

Peretz S, Regev O (2012). Carbon nanotubes as nanocarriers in medicine. Curr Opin Colloid Interf Sci 17: 360-368.

Pergantis SA, Jones-Lepp TL, Heithmar EM (2012). Hydrodynamic chromatography online with single particle-inductively coupled plasma mass spectrometry for ultratrace detection of metal-containing nanoparticles. Anal Chem 84: 6454-6462.

Petryayeva E, Algar WR (2014). Multiplexed homogeneous assays of proteolytic activity using a smartphone and quantum dots. Anal Chem 86: 3195-3202.

Petryayeva E, Algar WR, Medintz IL (2013). Quantum dots in bioanalysis: A review of applications across various platforms for fluorescence spectroscopy and imaging. Appl Spect 67: 215-252.

Piella J, Bastus NG, Puntes V (2016). Size-controlled synthesis of sub-10-nanometer citrate-stabilized gold nanoparticles and related optical properties. Chem Mater 28: 1066-1075.

Pieranski P (1983). Colloidal crystals. Contemp Phys 24: 25-73.

Pla-Roca M, Isa L, Kumar K, Reimhult E (2015). Selective (bio) functionalization of solid-state nanopores. Acs Appl Mater Interf 7: 6030-6035.

Pokhrel M, Mimun LC, Yust B, Kumar GA, Dhanale A, Tang L, Sardar DK (2014). Stokes emission in GdF3:$Nd3^{+}$ nanoparticles for bioimaging probes. Nanoscale 6: 1667-1674.

Polavarapu L, Perez-Juste J, Xu QH, Liz-Marzan LM (2014). Optical sensing of biological, chemical and ionic species through aggregation of plasmonic nanoparticles. J Mater Chem C 2: 7460-7476.

Prevo BG, Velev OD (2004). Controlled, rapid deposition of structured coatings from micro-and nanoparticle suspensions. Langmuir 20: 2099-2107.

Prorok K, Bednarkiewicz A, Cichy B, Gnach A, Misiak M, Sobczyk M, Strek W (2014). The impact of shell host (NaYF4/CaF2) and shell deposition methods on the up-conversion enhancement in $Tb3^{+}$, $Yb3^{+}$ codoped colloidal alpha-NaYF4 core-shell nanoparticles. Nanoscale 6: 1855-1864.

Qiu F, Chen Y, Tang C, Lu Y, Cheng J, Zhao X (2012). Formation of reversed micelle nanoring by a designed surfactant-like peptide. Nano 7: 1250024.

Rabarot M, Bablet J, Ruty M, Kipp M, Chartier I, Dubarry C (2003). Thick SU-8 photolithography for BioMEMS. P Soc Photo-Opt Ins 4979: 382-393.

Rodio M, Brescia R, Diaspro A, Intartaglia R (2016). Direct surface modification of ligand-free silicon quantum dots prepared by femtosecond laser ablation in deionized water. J Colloid Interf Sci 465: 242-248.

Ruhl T, Spahn P, Hellmann GP (2003). Artificial opals prepared by melt compression. Polymer 44: 7625-7634.

Samusev AK, Samusev KB, Rybin MV, Limonov MF, Trofimova EY, Kurdyukov DA, Golubev VG (2011). Two-dimensional light diffraction from thin opal films. Phys Solid State+ 53: 1056-1061.

Sapsford KE, Tyner KM, Dair BJ, Deschamps JR, Medintz IL (2011). Analyzing nanomaterial bioconjugates: a review of current and emerging purification and characterization techniques. Anal Chem 83: 4453-4488.

Schmidt S, Wang H, Pussak D, Mosca S, Hartmann L (2015). Probing multivalency in ligand-receptor-mediated adhesion of soft, biomimetic interfaces. Beilstein J Org Chem 11: 720-729.

Schwaminger SP, Garcia PF, Merck GK, Bodensteiner FA, Heissler S, Guenther S, Berensmeier S (2015). Nature of interactions of amino acids with bare magnetite nanoparticles. J Phys Chem C 119: 23032-23041.

Seisenbaeva GA, Daniel G, Nedelec JM, Gun'ko YK, Kessler VG (2012). High surface area ordered mesoporous nano-titania by a rapid surfactant-free approach. J Mater Chem 22: 20374-20380.

Shim SE, Cha YJ, Byun JM, Choe S (1999). Size control of polystyrene beads by multistage seeded emulsion polymerization. J Appl Poly Sci 71: 2259-2269.

Sicard C, Brayner R, Margueritat J, Hemadi M, Coute A, Yepremian C, Djediat C, Aubard J, Fievet F, Livage J et al. (2010). Nano-gold biosynthesis by silica-encapsulated micro-algae: a living bio-hybrid material. J Mater Chem 20: 9342-9347.

Siglreitmeier M, Wu B, Kollmann T, Neubauer M, Nagy G, Schwahn D, Pipich V, Faivre D, Zahn D, Fery A et al. (2015). Multifunctional layered magnetic composites. Beilstein J Nanotechnol 6: 134-148.

Skorb EV, Andreeva DV (2015). Self-healing properties of layer-by-layer assembled multilayers. Poly Int 64: 713-723.

Skorb EV, Moehwald H (2014). "Smart" surface capsules for delivery devices. Adv Mater Interf 1: 1400237.

Solans C, Sol I (2012). Nano-emulsions: formation by low-energy methods. Curr Opin Colloid Interf Sci 17: 246-254.

Spillmann CM, Naciri J, Anderson GP, Chen MS, Ratna BR (2009). Spectral tuning of organic nanocolloids by controlled molecular interactions. ACS Nano 3: 3214-3220.

Stachowski GM, Bauer C, Waurisch C, Bargheer D, Nielsen P, Heeren J, Hickey SG, Eychmueller A (2014). Synthesis of radioactively labelled CdSe/CdS/ZnS quantum dots for in vivo experiments. Beilstein J Nanotechnol 5: 2383-2387.

Subbiah R, Veerapandian M, Yun KS (2010). Nanoparticles: functionalization and multifunctional applications in biomedical sciences. Curr Med Chem 17: 4559-4577.

Sun FQ, Yu JC, Wang XC (2006). Construction of size-controllable hierarchical nanoporous TiO_2 ring arrays and their modifications. Chem Mater 18: 3774-3779.

Sun S, Murray C, Weller D, Folks L, Moser A (2000). Nanocrystal superlattices monodisperse FePt nanoparticles and ferromagnetic FePt. Science 287: 1989-1992.

Sun Z, Li Y, Zhang J, Li Y, Zhao Z, Zhang K, Zhang G, Guo J, Yang B (2008). A universal approach to fabricate various nanoring arrays based on a colloidal-crystal-assisted-lithography strategy. Adv Funct Mater 18: 4036-4042.

Sun ZQ, Chen X, Zhang JH, Chen ZM, Zhang K, Yan X, Wang YF, Yu WZ, Yang B (2005). Nonspherical colloidal crystals fabricated by the thermal pressing of colloidal crystal chips. Langmuir 21: 8987-8991.

Susumu K, Mei BC, Mattoussi H (2009). Multifunctional ligands based on dihydrolipoic acid and polyethylene glycol to promote biocompatibility of quantum dots. Nat Protoc 4: 424-436.

Susumu K, Uyeda HT, Medintz IL, Pons T, Delehanty JB, Mattoussi H (2007). Enhancing the stability and biological functionalities of quantum dots via compact multifunctional ligands. J Am Chem Soc 129: 13987-13996.

Tan LF, Wang SP, Xu K, Liu TL, Liang P, Niu M, Fu CH, Shao HB, Yu J, Ma TC et al. (2016). Layered MoS_2 hollow spheres for highly-efficient photothermal therapy of rabbit liver orthotopic transplantation tumors. Small 12: 2046-2055.

Tekin M, Hişmi Burcu Ö, Fitoz S, Özdağ H, Cengiz Filiz B, Sırmacı A, Aslan İ, İnceoğlu B, Yüksel-Konuk EB, Yılmaz Seda T et al. (2007). Homozygous mutations in fibroblast growth factor 3 are associated with a new form of syndromic deafness characterized by inner ear agenesis, microtia, and microdontia. Am J Hum Genet 80: 338-344.

Tielemans M, Roose P, De Groote P, Vanovervelt JC (2006). Colloidal stability of surfactant-free radiation curable polyurethane dispersions. Prog Org Coat 55: 128-136.

Tien J, Terfort A, Whitesides GM (1997). Microfabrication through electrostatic self-assembly. Langmuir 13: 5349-5355.

Trau M, Saville DA, Aksay IA (1996). Field-induced layering of colloidal crystals. Science 272: 706.

Unser S, Bruzas I, He J, Sagle L (2015). Localized surface plasmon resonance biosensing: current challenges and approaches. Sensors 15: 15684-15716.

Urban MW (2014). Stimuli-responsive colloids: from stratified to self-repairing polymeric films and beyond. Curr Opin Colloid Interf Sci 19: 66-75.

Vazquez-Gonzalez M, Carrillo-Carrion C (2014). Analytical strategies based on quantum dots for heavy metal ions detection. J Biomed Opt 19: 101503.

Velev O, Jede T, Lobo R, Lenhoff A (1998). Microstructured porous silica obtained via colloidal crystal templates. Chem Mater 10: 3597-3602.

Verderio P, Avvakumova S, Alessio G, Bellini M, Colombo M, Galbiati E, Mazzucchelli S, Avila JP, Santini B, Prosperi D (2014). Delivering colloidal nanoparticles to mammalian cells: A nano-bio interface perspective. Adv Health Mater 3: 957-976.

Vickreva O, Kalinina O, Kumacheva E (2000). Colloid crystal growth under oscillatory shear. Adv Mater 12: 110-112.

Vilela D, Cristina Gonzalez M, Escarpa A (2014). (Bio)-synthesis of Au NPs from soy isoflavone extracts as a novel assessment tool of their antioxidant capacity. RSC Advances 4: 3075-3081.

Wagner M, Holzschuh S, Traeger A, Fahr A, Schubert US (2014). Asymmetric flow field-flow fractionation in the field of nanomedicine. Anal Chem 86: 5201-5210.

Wagner M, Holzschuh S, Traeger A, Fahr A, Schubert US (2015). Heteroaggregation of nanoparticles with biocolloids and geocolloids. Adv Colloid Interf Sci 226: 24-36.

Wang Y, Schluecker S (2013). Rational design and synthesis of SERS labels. Analyst 138: 2224-2238.

Wen H, Meng L, Kong G, Yu H, Yang Z, Hu J (2014). Sub-5 nm nanobowl gaps electrochemically templated by SiO2-coated Au nanoparticles as surface-enhanced Raman scattering hot spots. Chem Commun 50: 3958-3961.

Xiao F (2012). An efficient layer-by-layer self-assembly of metal-TiO2 nanoring/nanotube heterostructures, M/T-NRNT (M = Au, Ag, Pt), for versatile catalytic applications. Chem Commun 48: 6538-6540.

Xiao M, Li Y, Allen MC, Deheyn DD, Yue X, Zhao J, Gianneschi NC, Shawkey MD, Dhinojwala A (2015). Bio-inspired structural colors produced via self-assembly of synthetic melanin nanoparticles. ACS Nano 9: 5454-5460.

Xing H, Li J, Guo J, Wei J (2015). Bio-inspired thermal-responsive inverse opal films with dual structural colors based on liquid crystal elastomer. J Mater Chem C 3: 4424-4430.

Xu W, Bai X, Xu S, Zhu Y, Xia L, Song H (2012). Remarkable fluorescence enhancement in YVO4:Eu3+@Ag nano-hybrids induced by interface effect. RSC Advances 2: 2047-2054.

Yallappa S, Manjanna J, Dhananjaya BL (2015). Phytosynthesis of stable Au, Ag and Au-Ag alloy nanoparticles using *J. sambac* leaves extract, and their enhanced antimicrobial activity in presence of organic antimicrobials. Spectrochim Acta Part A 137: 236-243.

Yallappa S, Manjanna J, Sindhe MA, Satyanarayan ND, Pramod SN, Nagaraja K (2013). Microwave-assisted rapid synthesis and biological evaluation of stable copper nanoparticles using *T. arjuna* bark extract. Spectrochim Acta Part A 110: 108-115.

Yang D, Tian H, Ji Y, Quan Q (2013). Design of simultaneous high-Q and high-sensitivity photonic crystal refractive index sensors. J Opt B-Quantum S O 30: 2027-2031.

Yang H, Gozubenli N, Fang Y, Jiang P (2013). Generalized fabrication of monolayer nonclose-packed colloidal crystals with tunable lattice spacing. Langmuir 29: 7674-7681.

Yang Q, Lan F, Yi Q, Wu Y, Gu Z (2015). A colloidal assembly approach to synthesize magnetic porous composite nanoclusters for efficient protein adsorption. Nanoscale 7: 17617-17622.

Yasun E, Gulbakan B, Ocsoy I, Yuan Q, Shukoor MI, Li C, Tan W (2012). Enrichment and detection of rare proteins with aptamer-conjugated gold nanorods. Anal Chem 84: 6008-6015.

Yasun E, Kang H, Erdal H, Cansiz S, Ocsoy I, Huang YF, Tan W (2013). Cancer cell sensing and therapy using affinity tag-conjugated gold nanorods. Interface Focus 3: 20130006.

Yasun E, Li C, Barut I, Janvier D, Qiu L, Cui C, Tan W (2015). BSA modification to reduce CTAB-induced nonspecificity and cytotoxicity of aptamer-conjugated gold nanorods. Nanoscale 7: 10240-10248.

Yokel R, Grulke E, MacPhail R (2013). Metal-based nanoparticle interactions with the nervous system: the challenge of brain entry and the risk of retention in the organism. Wiley Interdiscip Rev Nanomed Nanobiotechnol 5: 346-373.

Zeira A, Chowdhury D, Hoeppener S, Liu ST, Berson J, Cohen SR, Maoz R, Sagiv J (2009). Patterned organosilane monolayers as lyophobic-lyophilic guiding templates in surface self-assembly: monolayer self-assembly versus wetting-driven self-assembly. Langmuir 25: 13984-14001.

Zhang C, Zhu Y, Zhang R, Xie Y, Wang K, Liu X (2015). Pickering emulsions stabilized by composite nanoparticles prepared from lysozyme and dopamine modified poly (gamma-glutamic acid): effects of pH value on the stability of the emulsion and the activity of lysozyme. RSC Advances 5: 90651-90658.

Zhang L, Zhou JP, Huang J, Gong P, Zhou Q, Zheng LS, Du YM (1999). Biodegradability of regenerated cellulose films coated with polyurethane/natural polymers interpenetrating polymer networks. Ind Eng Chem Res 38: 4284-4289.

Zhang Z, Wang P (2012). Optimization of photoelectrochemical water splitting performance on hierarchical TiO2 nanotube arrays. Energ Environ Sci 5: 6506-6512.

Zhao J, Ma L, Millians W, Wu T, Ming W (2016). Dual-functional antifogging/antimicrobial polymer coating. ACS Appl Mater Interf 8: 8737-8742.

Zhong X, Han M, Dong Z, White TJ, Knoll W (2003). Composition-tunable $Zn_xCd_{1-x}Se$ nanocrystals with high luminescence and stability. J Am Chem Soc 125: 8589-8594.

Zhu X, Li J, He H, Huang M, Zhang X, Wang S (2015). Application of nanomaterials in the bioanalytical detection of disease-related genes. Biosens Bioelectron 74: 113-133.

Zhu X, Wang H, Jiao Q, Xiao X, Zuo X, Liang Y, Nan J, Wang J, Wang L (2014). Preparation and characterization of the fluorescent carbon dots derived from the lithium-intercalated graphite used for cell imaging. Part Part Syst Char 31: 771-777.

Zrazhevskiy P, Gao X (2013). Quantum dot imaging platform for single-cell molecular profiling. Nature Commun 4: 1619.

Zu X, Gong J, Tu W, Deng Y (2011). Selective and sequential re-assembly of patterned block copolymer thin film for fabricating polymeric, inorganic, and their composite nanostructured arrays. Macromol Rapid Comm 32: 1526-1532.